Research article

Encapsulation of *Apium graveolens* essential oil into chitosan nanobiopolymer for protection of stored rice against *Fusarium verticill i oides* and fumonisins contamination

Somenath Das [a,*], Anand Kumar Chaudhari [b]

[a] *Department of Botany, Burdwan Raj College, Purba Bardhaman, 713104, West Bengal, India*
[b] *Department of Botany, Rajkiya Mahila Snatkottar Mahavidyalaya, Ghazipur, Uttar Pradesh, 233001, India*

ARTICLE INFO

ABSTRACT

The present investigation entails the encapsulation of *Apium graveolens* essential oil into chitosan nanobiopolymer (AGEO-Ne) and assessment of its efficacy against *Fusarium verticill i oides* contamination and fumonisins biosynthesis in stored rice (*Oryza sativa* L.) samples. The AGEO was encapsulated through ionic gelation process and characterized by scanning electron microscopy (SEM), Dynamic light scattering (DLS), X-ray diffractometry (XRD), and Fourier transform infrared spectroscopy (FTIR) analyses. The AGEO exhibited bi-phasic delivery pattern from chitosan matrix. The AGEO caused complete inhibition of *F. verticill i oides* growth at 1.2 μL/mL, while fumonisin B_1 (FB_1) and B_2 (FB_2) biosynthesis at 1.2 and 1.0 μL/mL, respectively. On the other hand, nanoencapsulated AGEO (AGEO-Ne) exhibited improved efficacy, caused complete inhibition of fungal growth at 0.8 μL/mL, and FB_1 and FB_2 production at 0.8 and 0.6 μL/mL, respectively. AGEO-Ne caused 100 % inhibition of ergosterol synthesis at 0.8 μL/mL and exhibited greater efflux of Ca^{2+}, Mg^{2+}, K^+ ions (18.99, 21.63, and 25.38 mg/L) as well as 260 and 280 nm absorbing materials from exposed fungal cells. The *in silico* interaction of granyl acetate and linalyl acetate with FUM 21 protein validated the molecular mechanism for inhibition of FB_1 and FB_2 biosynthesis. Further, improvement in antioxidant activity of AGEO-Ne was observed after encapsulation with IC_{50} values of 12.08 and 6.40 μL/mL against DPPH and ABTS radicals, respectively. During *in situ* investigation, AGEO caused 82.09 and 86.32 % protection of rice against *F. verticill i oides* contamination in inoculated and uninoculated rice samples, respectively, while AGEO-Ne exhibited 100 % protection of fumigated rice samples against *F. verticill i oides* proliferation as well as FB_1 and FB_2 contamination. The AGEO-Ne also caused better retardation of lipid peroxidation (41.35 and 37.52 μM/g FW malondialdehyde in inoculated and uninoculated treatment) and acceptable organoleptic properties in rice samples, which strengthen its application as plant based novel preservative in food and agricultural industries.

1. Introduction

Mycotoxin contamination in rice during the storage conditions is a challenging issue throughout the world. Among different mycotoxins, fumonisins produced by *Fusarium verticill i oides* are of major concern because it has been associated with different animal

---

diseases including pulmonary edema, equine leukoencephalomalacia, and alteration of immunological parameters [1]. Approximately 30 different derivatives of fumonisin have been reported, among which B type fumonisins (FBs, especially FB_1 and FB_2) being the most common and most toxic type accounting for 70–80 % of all fumonisins contaminations in cereal and cereal based products [2]. Based on their toxicity, International Agency for Research on Cancer has classified them as class 2B carcinogen, a possible human carcinogen [3,4]. In human, liver and kidney are the most subtle targets of FBs; however, their exposure has been also linked to the defective development of neural tubes, growth impairment, cardiovascular diseases, and the prevalence of esophageal cancer [5].

Different strategies have been adopted to mitigate the proliferation of toxigenic fungi and fumonisin contamination, among them the chemical fungitoxicants are greatly employed for their inhibition. However, the indiscriminate use of these chemicals has increased the risk of residual toxicity along with damage of environmental integrity [6]. Several physical and biological methods are commonly employed to control fumonisin contamination, however, these process require sophisticated equipments and expensive reagents leading to their limited practical applications. Currently, cumulative interest has been gained on plant essential oils regarding inhibition of fungi and mycotoxin contamination in cereal grains [7]. Moreover, the essential oils are included in Generally Recognized as Safe category and possess strong antimicrobial potency and anti-mycotoxigenic activity [8]. However, the essential oils are associated with several factors such as high volatility, low aqueous phase solubility, less stability, and low antifungal potency in real food matrix which limits their practical application in food system. Hence, a relevant delivery vehicle is indispensable for improvement of the esteemed effects [9]. Recently, nanoencapsulation of essential oil into biocompatible polymer has been emerged as an innovative technique for controlled delivery in food system [10]. A recent investigation of Karami-Osboo et al. [11] suggested inhibition of *Aspergillus flavus* growth and reduced the level of aflatoxin B_1 by chitosan encapsulated *Zataria multiflora* essential oil in contaminated pistachio nut. The chitosan based encapsulation of *Toddalia asiatica* essential oil along with the enhancement in bioefficacy against *Aspergillus flavus* growth and mitigation of aflatoxin B_1 contamination in stored maize (*Zea mays* L.) samples has been demonstrated by Roshan et al. [12]. Kalagatur et al. [13] reported the antifungal activity of *Cymbopogon martinii* essential oil loaded chitosan nanoparticle against *Fusarium graminearum* infestation and deoxynivalenol and zearalenone contamination in stored maize samples. Among the nanoencapsulation approaches designed so far for entrapment of essential oils, ionic gelation is one of the best methods for nanoemulsion mediated delivery system with the utilization of chitosan as wall matrix and sodium tripolyphosphate (S-TPP) as cross linking agent [14].

Apium graveolens L. (Family: Apiaceae) is a common herbaceous annual plant with ridges and succulent branches. The dried fruits are mainly used in medicinal purposes to treat stomach problem, spasm, and also applied as heart tonic to reduce the blood pressure [15]. The *Apium graveolens* seed essential oil (AGEO) has been used to relief arthritic pain, rheumatism, and gout [16]. However, the application of AGEO loaded chitosan nanoemulsion against *Fusarium verticilli oides* contamination and fumonisin biosynthesis for protection of stored rice samples has not been elucidated till now.

The present research objective was encapsulation of AGEO within chitosan nanoemulsion (AGEO-Ne) by ionic gelation process and chemical characterization through Scanning electron microscopy (SEM), Dynamic light scattering (DLS), X-ray diffractometry (XRD), and Fourier transform infrared spectroscopy (FTIR) analyses. The release behavior was assessed to demonstrate the sustained delivery of AGEO. The antifungal and anti-fumonisin efficacy of AGEO-Ne was also evaluated along with its biochemical and molecular mechanism of action. Furthermore, the *in situ* inhibitory activity of AGEO-Ne against *Fusarium verticilli oides*, fumonisin contamination, and lipid peroxidation in stored rice samples along with evaluation of organoleptic properties was determined to recommend its potentiality as smart and nano-green preservative.

2. Materials and methods

2.1. Chemicals

Chemicals *viz.*, PDA (potato dextrose agar) (**P**otato 200 g; **D**extrose 20 g; **A**gar 15 g dissolved in 1000 mL distilled water) medium, acetonitrile, chloroform, methanol, toluene, Tween 20, Tween 80, ethanol, sodium tripolyphosphate, dichloromethane, petroleum ether, trichloroacetic acid, thiobarbituric acid, potassium hydroxides, acetic acid, ethyl acetate, n-hexane, acetone, potassium dihydrogen phosphate (KH_2PO_4), potassium monohydrogen phosphate (K_2HPO_4), DPPH, ABTS, potassium per sulfate ($K_2S_2O_8$), sodium hypochlorite (NaOCl), Folin's Ciocalteu's phenol reagent, and sodium chloride (NaCl) were required for the present study. They were purchased from HiMedia Pvt. Ltd., Mumbai and Sigma Laboratories, Bengaluru, India. We have collected low molecular weight chitosan (50–160 kDa) with deacetylation degree 75–80 % (CAS: 9012–76–4) from Sigma-Aldrich Chemicals Pvt. Ltd., Bengaluru, India. The purity grade of the chemicals was >98 %.

2.2. Fungal strain

The strain of *Fusarium verticilli oides* (producing fumonisin B_1 and B_2) has been isolated from the stored rice samples. Five varieties of rice samples were collected from different regions of India. Mycoflora analysis of rice samples showed 10 different *F. verticilli oides* strains. Among them, FV-BRC-05 showed maximum production of fumonisin B_1 and B_2 and has been selected as test strain for the present investigation (Authors unpublished work). Maintenance of fungal strain was performed at 4 °C at Potato dextrose agar (PDA) medium. For preparation of spore suspension, the disc of *F. verticilli oides* pure culture was aseptically inoculated in Petri plate having PDA medium and left in B·O.D incubator at 25 ± 2 °C for 10 days. After that, PDA surface having the fungal growth with spores was immersed into sterilized 0.1 % Tween-80 solution (prepared in double distilled water). Thereafter, the spores from *F. verticilli oides* were obtained by shaking the immersed PDA surface with spatula. The same procedure was repeated multiple times for maximum

collection of spores. Finally, the double distilled water containing fungal spores was filtered through double layered muslin cloth and suspended in 0.1 % Tween-80 solution in conical flask [17,18]. The spore density was measured as 1×10^6 spores/mL by hemocytometer.

2.3. Isolation and characterization of Apium graveolens essential oil (AGEO)

The fruits of *Apium graveolens* were collected from an agriculture farm of Durgapur, West Bengal, India. The fruits (500g) were submitted to hydrodistillation at 50 °C for 5 h using a Clevenger-type apparatus (Merck Specialities Pvt., Ltd., Mumbai, India). The essential oil was separated in graduated tube and collected over the anhydrous sodium sulfate to remove excess water. The collected essential oil was stored in clean amber vial at 4 °C in refrigerator for further experimental analyses. The AGEO was characterized through Gas chromatography Mass spectrometry (GC-MS) analysis. The analysis was performed by TG-5 MS silica capillary column fused with Thermo Scientific 1300 GC and TSQ quadruple Mass spectrometry. The AGEO was diluted 100 times in n hexane and 1 μL was injected under the consecutive points; oven temperature and injector temperature at 250 °C, and 60–240 °C which enhanced to 270 °C at a rate of 5 °C/min, Helium (He) was used as carrier gas with flow rate 1 mL/min, ion source and transfer line temperature 220 °C and 245 °C with energy of ionization 70 eV. The mass scan range was 40–450 amu. The components were identified by NIST (National Institute of Standards and Technology) and WILEY (Wiley online) libraries [19].

2.4. Synthesis of Apium graveolens essential oil infused chitosan nanoemulsion (AGEO-Ne)

Encapsulation of AGEO into chitosan nanobiopolymer was performed by ionic gelation technique of Hosseini et al. [20] with little changes. For this, 1.3 g of chitosan was mixed with 120 mL of double distilled water containing 1 % acetic acid and agitated for overnight on magnetic stirrer at 27 °C. Thereafter, tween-80 (450 mg) was dissolved into chitosan solution and again vortexed for 2 h (45 °C). Specific amounts of AGEO were dissolved into 3.5 mL of dichloromethane to develop the oil phase and subsequently added to the solution of chitosan at high speed homogenization of 12,960×g for 15 min at 4 °C for the development of oil-in-water emulsion. After that, 0.35 g of sodium-tripolyphosphate (S-TPP) was inflated to the emulsion for ionic gelation and agitated for 40 min at 25 °C. The synthesized emulsionic particles were collected by centrifugation at 12,560×g for 14 min. Subsequently, isolated pellet was repeatedly washed by tween-80 for 3 times and finally diffused to 10 mL of double distilled water followed by sonication for 4 min to develop AGEO loaded chitosan nanoemulsion (AGEO-Ne). Similar process was used to develop chitosan nanoemulsion (CS-Ne) without involving AGEO.

2.5. Entrapment (EE) and loading efficiency (LE) of AGEO-Ne

For this, 200 μL of AGEO-Ne was mixed with 3 mL of ethyl acetate (added in a sequence of 1 + 1 + 1 mL) and subjected to centrifugation at 10,690×g for 13 min. The supernatant was used to determine EE and LE of AGEO-Ne through standard curve of AGEO prepared at 268 nm (Y = 0.0236 X + 0.0063; R^2 = 0.987). A blank without mixing of AGEO-Ne was also prepared in the same way. Following formula was used for determination of EE and LE of AGEO-Ne [21].

$$EE\ (\%) = \frac{\text{Amount of loaded AGEO in nanoemulsion}}{\text{Initial amount of AGEO added}} \times 100 \tag{1}$$

$$LE\ (\%) = \frac{\text{Amount of loaded AGEO in nanoemulsion}}{\text{Weight of nanoemulsion}} \times 100 \tag{2}$$

Amount of AGEO loaded in nanoemulsion was determined by putting the absorbance value of supernatant (as recorded at 268 nm) in the standard curve followed by multiplication with the dilution factor. This value provides the total amount of loaded AGEO. When the "total amount of loaded AGEO (value expressed as μL)" was divided by "initial amount of AGEO applied (value expressed as μL)" during the homogenization process it has given the entrapment efficiency (%). However, the "total amount of loaded AGEO (value expressed as μL)" was divided by "total weight of nanoemulsion" (value has been converted to μL from mL) it has provided the loading efficiency (%).

2.6. Physico-chemical characterization of AGEO-Ne

2.6.1. Dynamic light scattering (DLS)
Particle size distribution of CS-Ne and AGEO-Ne was determined by DLS technique using a zetasizer (Malvern Instrument, Worcestershire, UK). Different size criteria of CS-Ne and AGEO-Ne were particle size, zeta potential, and polydispersity index (PDI). To achieve this, 0.001 mL of sample was dissolved in 10 mL of double distilled water and performed in presence of laser wavelength 532 nm and scattering angle of 173° at 25 °C [22].

2.6.2. Scanning electron microscopy (SEM)
The morphological structure of CS-Ne and AGEO-Ne was determined by SEM analysis. For this, 1 mL of CS-Ne and AGEO-Ne emulsion was dissolved in 10 mL of double distilled water and sonicated for 5 min. Thereafter, one drop of the dispersion was spread on a glass slide, dried and mounted on an aluminium stub followed by thin layer of gold coating using a vacuum dependent ion

sputtering (E−1010, Hitachi, Japan). Thereafter, the gold coated samples were observed in scanning electron microscope (EVO 18 Research, Zeiss, Germany) at 30 KX magnification.

2.6.3. Peak structure analysis by fourier transform infrared spectroscopy (FTIR)
The FTIR analysis was conducted for chitosan, CS-Ne, AGEO, and AGEO-Ne by Fourier transform infrared spectroscopy (Perki-nElmer, USA). For this, the samples were grinded in potassium bromide (KBr) and pressed to form pellets. The spectra were obtained between 500 and 4000 cm^{-1} wave number (32 scan turns and 8 cm^{-1} resolution).

2.6.4. X-ray diffractometry (XRD) study
The XRD analysis representing the crystallographic structure of chitosan, CS-Ne, and AGEO-Ne were achieved by Bruker D8 diffractometer and operated at 40 KV. The scanning was performed over the range of 2θ angle 5–50° with a scanning of 0.05° min^{-1} and step angle 0.02° min^{-1} at room temperature.

2.7. Release structure of AGEO

The release structure of AGEO from chitosan nanoemulsion was studied in phosphate buffer saline (PBS; pH 7.0) according to the protocol of Esmaeili and Asgari [23] with little changes. Five hundred microlitre of AGEO-Ne was centrifuged at 9200×g for 12 min at 25 °C. After decanting water, 800 μL of PBS was added into microcentrifuge tube followed by agitation and incubation at ambient temperature for 7 days. At different interval of time (4 h of interval up to 1 day and after that 24 h of interval up to 7 days), centrifugation of the sample was performed at 8500×g for 15 min and a specified amount of supernatant (200 μL) was used for the release study. The fresh PBS was used to conserve the sink volume. The AGEO release amount was calculated by UV–Visible spectrophotometry (Hitachi 2900) at 275 nm using the calibration curve (Y = 0.216 X + 0.0034; R^2 = 0.9953) and cumulative amount released was measured using following formula.

$$\% \text{ Cumulative AGEO release} = \frac{\text{Cumulative release of AGEO at each sampling time}}{\text{Initial weight of AGEO loaded in the sample}} \times 100 \qquad (3)$$

2.8. Effectiveness for mitigation of F. verticill i oides proliferation and FB$_1$ and FB$_2$ synthesis by AGEO and AGEO-Ne

Required concentrations of AGEO (0.2–1.2 μL/mL) and AGEO-Ne (0.2–0.8 μL/mL) was dissolved into 9.5 mL of PDA and consequently 2 mm peripheral disc of *F. verticill i oides* was introduced to PDA. The control sets did not include AGEO and AGEO-Ne. All the sets were subjected to incubation at 27 ± 2 °C for 7 days. The AGEO and AGEO-Ne concentrations representing cent percent inhibition of *F. verticill i oides* growth were recognized as minimum inhibitory concentrations (MICs) [21].

For determination of FB$_1$ and FB$_2$, all the sets (control and treatment) were incubated for 5 days at 20 ± 2 °C. At the end of the incubation periods, all the plates were transferred into refrigerator at 4 °C for 10 days. The agar medium having mycelium was cut into small pieces (1 cm^2) and subjected to mix with 50 mL of 96 % methanol followed by agitation in a rotary shaker at 200×g for 24 h and filtered through filter paper (Whatman No. 1). The residue was then washed through 25 mL of methanol. Thereafter, the methanolic extracts were combined, dried over anhydrous sodium sulfate and evaporated to dryness at room temperature. The thin layer chromatographic technique was adopted for determination of FB$_1$ and FB$_2$. The crude extract (10 μL) was spotted onto a TLC plate (aluminium sheet, silica gel; Merck) along with 5 μg FB$_1$ and FB$_2$ standard. The spots were dried and developed into 96 % methanol/water (80:20 v/v). The plates were viewed after spraying with *p*-anisaldehyde (0.5 g *p*-anisaldehyde in methanol-acetic acid-sulfuric acid; 8:10:5 v/v/v) under UV-trans-illuminator (Zenith Engineers, India) under short-wave (254 nm) and long-wave (365 nm) UV irradiation. The FB$_1$ and FB$_2$ appeared as slight bluish green spots with Rf value 0.25 and 0.30, respectively [24,25].

2.9. The mechanisms of antifungal action

2.9.1. Effect on ergosterol production
The ergosterol content of *F. verticill i oides* was determined through the designed protocol of Sun et al. [26]. For this, the mycelia of AGEO and AGEO-Ne treated *F. verticill i oides* was mixed with 90 % ethanol and 15 % sodium hydroxide followed by heating at 80 °C for 2 h. Sterol was extracted by addition of petroleum ether (5 mL) and dried in N$_2$ steam. The absorbance of ergosterol and 24,28 dehydroergosterol was measured at 281.5 and 230 nm, respectively. Ergosterol amount was calculated by the following equation.

$$\% \text{ Ergosterol} = \frac{100}{1 + \frac{Absorbance\ at\ 230\ nm}{Absorbance\ at\ 281.5\ nm} \times 0.56} \qquad (4)$$

$$\% \ 24, 28 \text{ dehydroergosterol} = 100 \% \ - \ \% \text{ Ergosterol} \qquad (5)$$

2.9.2. Effect on ions, nucleic acid, and protein leakage
The method of Dwivedy et al. [27] was used to determine the leakage of ions, nucleic acids, and proteins from *F. verticill i oides* cells. The 10 days grown biomass of *F. verticill i oides* was isolated and washed twice by sterile distilled water. Thereafter, the biomass was suspended in 20 mL of 0.85 % NaCl solution followed by fumigation with different concentrations of AGEO (0.2–1.2 μL/mL) and

AGEO-Ne (0.2–0.8 μL/mL). The control sets did not include AGEO and AGEO-Ne fumigation in *F. verticill i oides* biomass. Thereafter, both the control and treatment sets were incubated for 24 h at 27 ± 2 °C. After completion of incubation period, the biomass was again filtered and filtrate was used for determination of leakage of Ca^{2+}, Mg^{2+}, and K^+ ions by Atomic absorption spectroscopy (PerkinElmer Aanalyst 800). However, absorbance of the filtrate at 260 nm and 280 nm was recorded by UV–Visible spectroscopy to determine the leakage of nucleic acids and proteins [28].

2.10. Anti-fumonisin mechanism of action of AGEO: In silico investigation

The molecular docking study was performed using a combination of bioinformatic tools like PatchDock, FireDock, Chimera 1.8.1. and Discovery studio 4.0 software. The FASTA sequence of FUM-21 protein was downloaded from UniProtKB software and developed the three dimensional (3 D) structure by Phyre 2 Protein fold Recognition server. The modeled FUM-21 protein was further refined by non-standard residues and addition of hydrogen. Functional and conservative residue of FUM-21 has been elucidated by CornSurf Web server. The 3 D structures of linalyl acetate and geranyl acetate (major components of AGEO) were retrieved from PubChem data base. Thereafter, the binding of ligand (linalyl acetate and geranyl acetate) and receptor (FUM-21 protein) was performed by PatchDock software and refined by FireDock software to get 10 best models on the basis of interactive energy like global energy, attractive vander waal force, and atomic contact energy. The results were ranked on the minimum global binding energy of the ligand receptor bond. To determine the ligand-receptor interaction Chimera 1.8.1 and Discovery Studio 4.0 Client were used [29].

2.11. Antioxidant potency and total phenolic content of AGEO and AGEO-Ne

2.11.1. 2,2-Diphenyl-1-picrylhydrazyl (DPPH) radical scavenging assay

Briefly, different concentrations of AGEO (5.0–30 μL/mL) and AGEO-Ne (2.0–20 μL/mL) were dissolved in 2 mL of 0.004 % methanolic DPPH solution [14]. The mixture was incubated at room temperature for 20 min and then optical density was measured at 517 nm against a blank by UV–Visible spectrophotometer. The radical quenching capability was measured by the following equation.

$$\% \text{ Radical quenching capability} = \frac{\text{Blank optical density} - \text{Sample optical density}}{\text{Sample optical density}} \times 100 \qquad (6)$$

In case of blank, methanol was used. The 50 % radical quenching capability of AGEO and AGEO-Ne was measured as IC_{50} value.

2.11.2. 2,2′-Azinobis-3-ethylbenzothiazoline-6-sulfonic acid (ABTS) radical scavenging assay

Preparation of ABTS radical solution was done by mixing of 0.0074 mol/L ABTS and 0.0026 mol/L potassium persulfate [30]. Different concentrations of AGEO (5.0–30 μL/mL) and AGEO-Ne (2.0–20 μL/mL) were homogenized into 1900 μL of ABTS radical solution and optical density was noted after incubation in dark (6 min) at 734 nm. Radical quenching capability was measured through DPPH equation.

2.11.3. Folin–Ciocalteu assay for total phenolic content determination

Total phenolic content of AGEO and AGEO-Ne was determined by spectrophotometric method of Folin–Ciocalteu assay following the protocol of Gholivand et al. [31]. A solution (0.1 mL) was prepared in conical flask containing 1000 μg of AGEO and AGEO-Ne and mixed with 46 mL of sterilized distilled water and 1 mL Folin–Ciocalteu reagent. The mixture was thoroughly agitated for 3 min and 3 mL of 2 % Na_2CO_3 solution was added followed by incubation at 25 ± 2 °C for 2 h. Absorbance of the mixture was measured at 760 nm. The same process was applied for gallic acid for development of standard curve and total phenolic content was determined by the equation expressed as μg gallic acid equivalent/mg of the oil.

$$\text{Absorbance} = 0.0012 \times \text{gallic acid (μg)} + 0.024 \qquad (7)$$

2.12. In situ efficacy of AGEO and AGEO-Ne for protection of rice: antifungal and anti-fumonisin activity

The *in situ* efficacy of AGEO and AGEO-Ne against the fungal infestation and fumonisin production into rice samples in storage containers was performed following the strategy of Mishra et al. [32]. Before experiment, the rice samples were sanitized by 1 % sodium hypochlorite solution (45 s at room temperature) followed by washing of three times with double distilled water under the aseptic conditions to remove the surface microbial contaminations. Thereafter, the experiment was performed in six different sets.

i) Uninoculated control (only rice seeds without inoculation of *F. verticill i oides* spore suspension and without fumigation of AGEO and AGEO-Ne) (UIC)
ii) Inoculated control (rice seeds inoculated with *F. verticill i oides* spore suspension and without fumigation of AGEO and AGEO-Ne) (IC)
iii) Uninoculated treatment with AGEO (rice seeds without inoculation of *F. verticill i oides* spore suspension and fumigated with AGEO) (U-AGEO-t)
iv) Inoculated treatment with AGEO (rice seeds inoculated with *F. verticill i oides* spore suspension and fumigated with AGEO)

v) Uninoculated treatment with AGEO (rice seeds without inoculation of *F. verticill i oides* spore suspension and fumigated with AGEO-Ne) (U-AGEO-Ne-t)

vi) Inoculated treatment with AGEO-Ne (rice seeds inoculated with *F. verticill i oides* spore suspension and fumigated with AGEO-Ne)

500 g of rice samples of each set was kept separately in clean and sterilized glass containers of 1 L capacity. The fungal inoculated rice sets (inoculated control and treatments) were introduced with 1 mL of *F. verticill i oides* spore suspension (1×10^6 spores mL^{-1}) by uniform spraying. The spore suspension of *F. verticill i oides* was prepared in 0.1 % tween-80. The treatment sets (uninoculated and inoculated treatment) were fumigated with AGEO and AGEO-Ne at the respective MIC doses i.e. 1.2 and 0.8 μL/mL, respectively. For fumigation, the required amount of AGEO (1.2 μL/mL) and AGEO-Ne (0.8 μL/mL) was calculated on the basis of the aerial volume of the storage container, and soaked separately onto a cotton swab ($2 \times 2 \times 1$ cm) to obtain the dose of minimum inhibitory concentrations and placed beneath the lid of the glass container. All the containers were kept air tight and stored for 1 year in the storage chamber at 27 ± 2 °C (relative humidity $\sim$ 70 %).

The samples of control and treatment sets stored for 1 year were then carried forward for mycological analysis by serial dilution method. The samples were individually ground in mixer grinder and before and after grinding, the blender's cup was rinsed with 90 % ethanol. The powdered samples were sieved through muslin cloth and 10 g of powder of each set was mixed with 90 mL of sterilized distilled water and homogenized for 15 min in a shaker. After that, 10 fold dilutions were prepared and 1 mL of 10^{-4} dilution was aseptically spread on PDA medium. The dilution was uniformly spread over the PDA medium by L shaped spreader and plates were incubated at 27 ± 2 °C for 10 days. The colony count of *F. verticill i oides* was made after 10 days and log cfu/g was calculated. Percent protection of rice samples was determined by the given formula.

$$\% \text{ Protection} = \frac{\text{Total } \frac{\text{cfu}}{\text{g}} \text{ of } F.verticillioides \text{ in control set} - \text{Total } \frac{\text{cfu}}{\text{g}} \text{ of } F.verticillioides \text{ in treatment set}}{\text{Total } \frac{\text{cfu}}{\text{g}} \text{ of } F.verticillioides \text{ in control set}} \times 100 \quad (8)$$

For quantification of fumonisin content, 10 g of milled samples was mixed with 50 mL of reaction mixture consisting of methanol, water, and acetonitrile (25:50:25 v/v/v) followed by 1 h of agitation and filtration through Whatman No. 1 filter paper. Thereafter, 10 mL of extraction was diluted by 40 mL of PBS and Whatman GF/A filter paper was used for further filtration. After that, 10 mL of diluted extract was purified through column chromatography (Fumonitest™ type of column from VICAM, Watertown, MA) at a flow rate of about 1–2 drops/second. The column was washed with 10 mL PBS followed by 2 mL water at a flow rate of 1–2 drops/second until air came through the column and the elute was discarded. The eluted sample (800 μL) was further dried under a nitrogen stream at 60 °C, and dissolved into 0.25 mL water and acetonitrile (70:30 v/v) by mixing in a vortex mixture for 1 min and retained at 4 °C until HPLC analysis [33]. Thereafter, 2 μL of sample was introduced into HPLC column and compared with a calibration curve of FB$_1$ and FB$_2$ standard. The HPLC determinations of rice samples were carried out at C18 (150×4.6 mm, 5 μm) column (Waters, Bengaluru, India) preceded by a 0.5 μm Rheodyne guard filter. The fluorometric detector of Prostar 363 module and star data system version 6.20 was used for the study. The mobile phase consisted of a mixture of acetonitrile, water and glacial acetic acid (30:69:1; v/v/v) with a flow rate of 1 mL/min. The stock solution of FB$_1$ and FB$_2$ was prepared in acetonitrile and water (50:50 v/v). Required amount of stock solution were then dried and mixed with acetonitrile and water (70:30 v/v/) to obtain the standard solution for HPLC calibration. The linearity of the analytical response was observed by using a calibration curve in the range of 0.1–1.0 ng/μL of FB$_1$ and FB$_2$ and the content was measured by μg/kg of rice seeds [24].

2.13. Lipid peroxidation inhibitory potency of AGEO and AGEO-Ne

The method of Das et al. [35] was used for estimation of lipid peroxidation in terms of malondialdehyde (MDA) content. Briefly, 0.056 g of milled rice samples were homogenized into hydrocholic acid inflexed thiobarbeturic acid and trichloroacetic acid solution (2.5 N HCl + 20 % TCA + 0.5 % TBA) and heated on waterbath at 70 °C for 22 min. After cooling, samples were centrifuged at $6500 \times g$ for 12 min and optical density of the supernatant was taken at 532 and 600 nm by UV–Visible spectrophotometry. MDA content (μM/g FW of rice) was calculated by the help of extinction coefficient of 1.56×10^5 M^{-1} cm^{-1}.

2.14. Determination of organoleptic qualities of rice

Different organoleptic parameters like color, texture, odor, and flavor were taken into consideration during fumigation of rice samples by AGEO and AGEO-Ne. Twenty different panelist (10 male and 10 female) from our institution (approved by ethical committee of Burdwan Raj College No. BRC-205632) were involved to assess the quality of different sensory parameters. The panelist signed a consent form pertaining to the testing of nanoemulsion treated rice. Five minutes were given to each panelist with 2 min rest to test the rice samples. The sensory properties were scored according to the 5 point hedonic scale viz. 1 = dislike extremely; 2 = dislike moderately; 3 = neither like nor dislike; 4 = like moderately; 5 = like extremely [36].

2.15. Statistical analysis

All the experiments were performed in triplicate and data analysis was done by mean $\pm$ standard error subjected to one way analysis of variance (ANOVA). Means were separated by Tukey's multiple comparison tests when ANOVA was significant (p $\leq$ 0.05)

(SPSS 10.0; Chicago, IL, USA).

3. Results and discussion

3.1. Isolation and characterization of AGEO

The AGEO was isolated from the fruits of *Apium graveolens*. The AGEO was chemically characterized through GC-MS analysis. Twenty three different components were identified and accounted 93.7 % of total oil (Table 1). Among different identified components, linalyl acetate (37.5 %), geranyl acetate (24.7 %), 1,8-cineol (8.9 %), and linalool (6.8 %) were recorded as the major ingredients of AGEO. Our result shows similarity to the previous investigation of Das et al. [37] for the chemical profiling of AGEO. Dabrowska et al. [38] reported very low content of linalool (0.1 %) from *Apium graveolens* essential oil. However, Hassanen et al. [39] reported D-limonene as the principal compound of AGEO. Variation in compounds of essential oil may depend on growing season, weather condition, harvesting time and chemotype of the plants [40]. Moreover, the plant developmental stage resulting from the interaction of physiological, biochemical, ecological, and evolutionary processes might be a possible reason for variation in essential oil composition [41]. Hence, chemical component analysis of essential oil is important before preparation of antifungal nanoformulations.

3.2. Entrapment (EE) and loading efficiency (LE) of AGEO-Ne

The entrapment and loading efficiency of AGEO-Ne is presented in Table 2. The EE value was increased from 29.67 to 95.23 % at different ratio of chitosan to AGEO ranging from 1:0.2 to 1:1. Similarly, the LE value was also found to increase from 0.37 to 5.64 % with rising chitosan to AGEO ratio from 1:0.2 to 1:1. The result was similar to the research of Chaudhari et al. [42] with increasing the value of EE (45.81–85.84 %) and LE (0.68–8.26 %) for Allspice essential oil during encapsulation into chitosan biopolymer. Interestingly, the present report showed better entrapment efficiency of AGEO into chitosan matrix. The variation in loading and entrapment efficiency has been associated with deacetylation degree of chitosan and essential oil affinity towards the wall matrix [43]. Moreover, the differences in entrapment and loading efficiency of essential oil also depend on types and composition of wall material, ratio of the essential oil to biopolymer matrix, physico-chemical properties and stability of the nanoemulsion [44]. The ratio of essential oil with wall matrix had a significant effect on encapsulation of essential oil. It has been reported that the smaller size of particles had the inconsiderable surface oil content which could be explained by droplet size [45]. In previous studies of Padua et al. [46] and Omar et al. [47] considerably low levels of encapsulation efficiency have been recorded during entrapment of essential oil and flax oil into zein particles which was also depend on the characteristic structure of biopolymer. Most notably, the high value of EE and LE is a desirable feature in encapsulation strategy because it improves the shelf-life of essential oil into nanoparticles [48]. The encapsulation improves the stability of the essential oil by protecting them from the fluctuating environmental conditions hence inhibits the oxidation and volatilization which directly helps in improvement of shelf life of essential oils [49,50].

Table 1
GC-MS analysis of *Apium graveolens* essential oil.

S.No.	Retention time (min)	Components	% Area	Retention index
1.	4.21	α-pinene	0.5	939
2.	4.52	Camphene	0.5	954
3.	5.02	Sabinene	tr	975
4.	6.09	1,4 cineol	tr	1014
5.	6.28	O-cymene	0.1	1026
6.	6.34	Sylvestrene	0.3	1030
7.	6.48	1,8 cineol	8.9	1031
8.	7.13	Lavender lactone	4.8	1039
9.	8.56	Linalool	6.8	1096
10.	9.73	1,2 dihydrolinalool	0.1	1135
11.	10.15	Camphor	2.9	1146
12.	11.06	Borneol	0.2	1169
13.	11.92	α-terpineol	0.5	1188
14.	13.47	Nerol	0.1	1229
15.	14.33	**Linalyl acetate**	37.5	1257
16.	15.56	Bornyl acetate	0.2	1285
17.	15.88	Trans sabinyl acetate	5.1	1290
18.	18.04	α-terpinyl acetate	0.1	1349
19.	19.43	**Geranyl acetate**	24.7	1381
20.	23.08	ar-curcumene	0.1	1480
21.	24.01	(Z)-α-Bisabolene	tr	1507
22.	25.63	Z- Nerolidol	0.1	1532
23.	26.96	Caryophyllene oxide	0.2	1583
		Total	93.7	

Note: Compounds in bold are major components.
tr = trace components (<0.1 %).

Table 2
Entrapment and loading efficiency of AGEO-Ne.

Chitosan/AGEO (w/v)	Entrapment efficiency (%)	Loading efficiency (%)
1:0.0	0.00 ± 0.00^a	0.00 ± 0.00^a
1:0.2	29.67 ± 1.63^b	0.37 ± 0.08^b
1:0.4	43.06 ± 3.08^c	1.24 ± 0.11^c
1:0.6	71.54 ± 4.16^d	2.97 ± 0.39^d
1:0.8	84.19 ± 2.07^e	4.09 ± 1.12^e
1:1	95.23 ± 4.14^f	5.64 ± 1.37^f

Note: Values are mean (n = 3) $\pm$ SE. The means followed by same letter in the same column are not significantly different according to ANOVA and Tukey's multiple comparison tests.

3.3. Physico-chemical characterization of AGEO-Ne

3.3.1. Dynamic light scattering

The mean diameter of CS-Ne was 28.32 nm while the diameter of AGEO-Ne was significantly increased and the size was detected as 89.86 nm (Fig. 1 A). The result of the present investigation is corroborated with the report of Hadidi et al. [51] suggesting increment in size of chitosan nanoparticles (265.1–444.5 nm) after entrapment of varying amounts of clove essential oil. Zeta potential has been identified as an important marker to detect the surface charge and stability of nanoparticles in suspension [52]. Gravitation, electrostatic interaction, and repulsion between the particle's surface charges resulted flocculation, aggregation, and dispersion. In the present study, the zeta potential of CS-Ne and AGEO-Ne were positive which reflected the stability of nanoemulsion system. The zeta potential of CS-Ne was found to be +35.21 mV while the encapsulation of AGEO declined the zeta potential to +28.97 mV (Fig. 1 B) which suggested the nanoparticles scattering in water. The decline in zeta value may be due to adsorption of AGEO on the surface of the particles which lead to masking of chitosan's amino groups [53]. In a similar manner, Keawchaoon and Yoksan [54] observed that the zeta value was reduced by addition of carvacrol which supported our present findings. PDI demonstrates the distribution of particles in emulsion medium. The PDI of CS-Ne was found to be 0.310 while incorporation of AGEO into chitosan nanobiopolymer lowered the PDI value to 0.245 (Fig. 1C). Lower value of PDI reflects particle homogeneity suggesting uniformity in diameter [55]. Hadidi et al. [51] also reported the decrement in PDI value from 0.337 to 0.117 after incorporation of clove essential oil into chitosan nanoparticles. Hence, AGEO-Ne particles with uniform size shows possible insights for better agricultural perspectives with fumonisins mitigation property.

#### 3.3.2. Scanning electron microscopy

The CS-Ne and AGEO-Ne particles are chiefly spherical to somewhat elongated in shape with smooth walled structure. The particle size of CS-Ne ranged between 13.19 - 26.29 nm while the AGEO-Ne particles fall in the range of 67.21–98.56 nm (Fig. 1 D, E). The enhanced size of AGEO-Ne has been linked with the entrapment of AGEO into chitosan nanomatrix [56]. The enhancement in particle size of AGEO-Ne as recorded in SEM investigation is in line with the report of DLS based particle size analyzer. However, minor variation in particle size has been associated with the instrumental sensitivity. The finding of the present investigation is in agreement to the report of Mondéjar-López et al. [57] for enhancement in particle size after encapsulation of garlic essential oil into chitosan nanoparticles. However, aggregation of CS-Ne and AGEO-Ne particles were observed at some places which is possibly associated with melting and combining effect of particles during ionic gelation process [23].

3.3.3. Fourier transform infrared spectroscopy

FTIR is an important characterization process for identification of functional groups associated with the interaction of chitosan, AGEO, and S-TPP. Chitosan displayed distinct peaks at 1070 (stretching of C–O bond), 1350 (amide III), 1600 (amide II), 1660 (amide I), 2870 (–CH bond stretching), and 3340 (–NH$_2$ bond stretching) [58] (Fig. 1 F). CS-Ne was developed by *trans*-linking interaction of chitosan and S-TPP which has been linked with transfer of amide peaks. The figure presented shifting of 1660 cm^{-1} peak to 1647 cm^{-1} affirming the cross-linking reaction in CS-Ne. Most notably, a new peak was recorded at 1560 cm^{-1} implying the electrostatic interaction of –NH$_3^+$ group of chitosan with phosphate groups of S-TPP developing the complex structure [59]. The AGEO exhibited peaks at 635 (N–H group stretching), 725 (C–H bending), 908, 1107 (C–O–C stretching), 1455 (C=C bending), 1585 (C–C aromatic ring), 1649 (C–H stretching), 1740 (C=O stretching), 2880 (-CH$_3$ group bending), 2920 (C–H stretching), and 3414 (-OH stretching) cm^{-1}. This might be due to the presence of a variety of bioactive components in EO, as already verified through GC-MS analysis. Further, majority of the peaks observed in CS-Ne and AGEO with slight shifts in wave number were recorded in AGEO-Ne (Fig. 1 F), which might be attributed to the possible chemical interactions between the amine groups of chitosan and phosphate groups of cross-linking agent S-TPP [60]. The above result demonstrated that AGEO was successfully entrapped into the chitosan polymer.

3.3.4. X-ray diffractometry study

Fig. 1 G demonstrates the diffraction pattern of chitosan, CS-Ne, and AGEO-Ne. The chitosan showed sharp peak at 2θ value 20° suggesting high degree of crystallinity. For CS-Ne, the XRD pattern showed broadening of peak caused by electrostatic interaction of chitosan with S-TPP resulting in the formation of amorphous structures [61]. However, the encompassment of AGEO within chitosan matrix caused maximum disarray in chitosan structural alignment with reduction in intensity of peak and widening of the peak area [20]. The finding revealed the successful encapsulation of AGEO into chitosan nanoemulsion. The result of the present investigation is
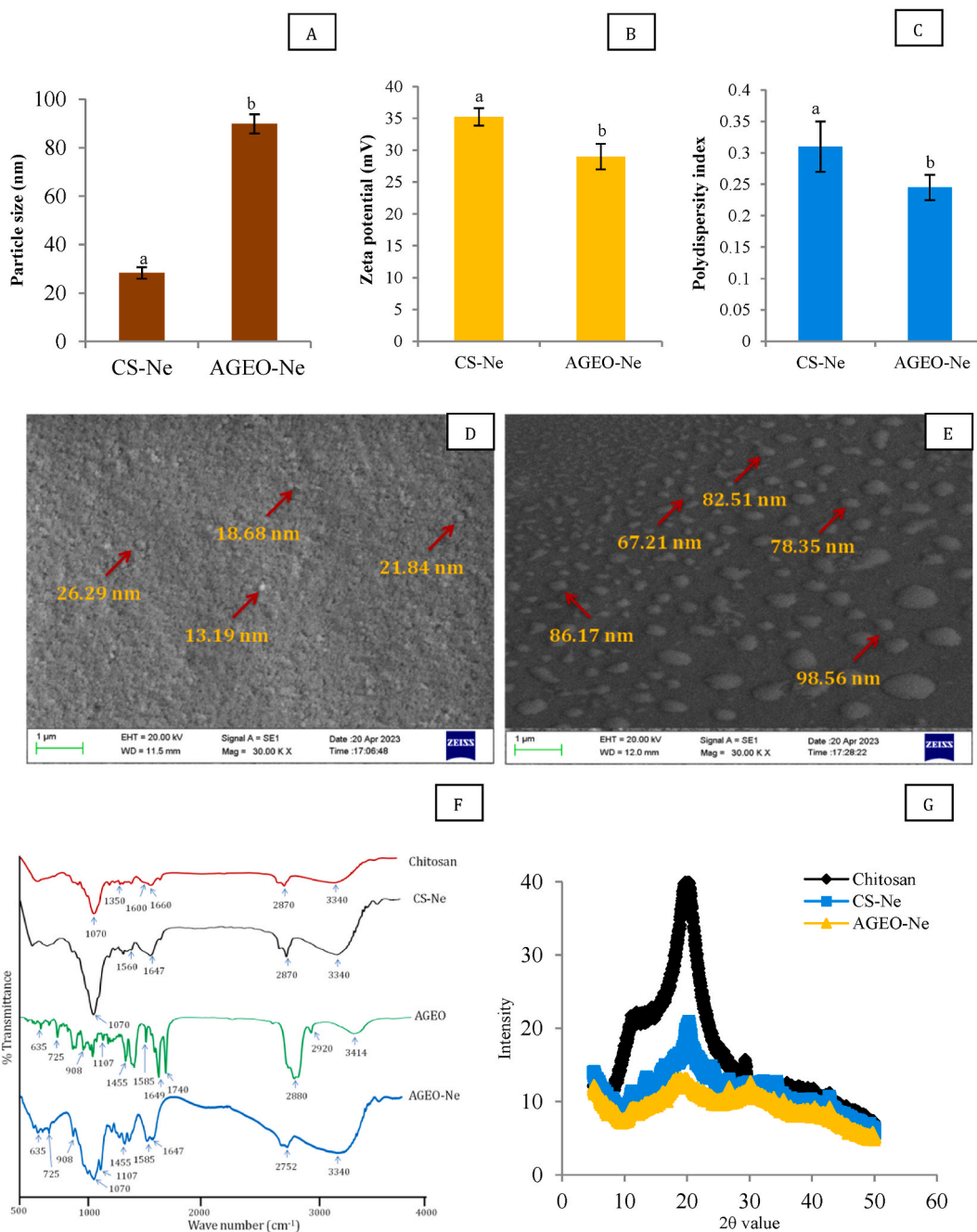
Fig. 1. (A) Particle size of CS-Ne and AGEO-Ne, (B) Zeta potential of CS-Ne and AGEO-Ne, (C) Polydispersity index of CS-Ne and AGEO-Ne, [Values are mean (n = 3) ± SE; different letters represent significant differences at p value ≤ 0.05 according to ANOVA and Tukey's multiple comparison tests.] (D) SEM image of CS-Ne, (E) SEM image of AGEO-Ne, (F) FTIR of chitosan, CS-Ne, AGEO, and AGEO-Ne, (G) XRD of chitosan, CS-Ne, and AGEO-Ne.

in agreement with the report of Hadidi et al. [51] suggesting the destruction in chitosan crystalline structure by S-TPP mediated cross-linking interaction and change in complex structure of S-TPP-chitosan by incorporation of clove essential oil in chitosan nanobiopolymer.

3.4. Release structure of AGEO

The result of AGEO release from chitosan nanobiopolymer is shown in Fig. 2 A. The release study was performed in phosphate
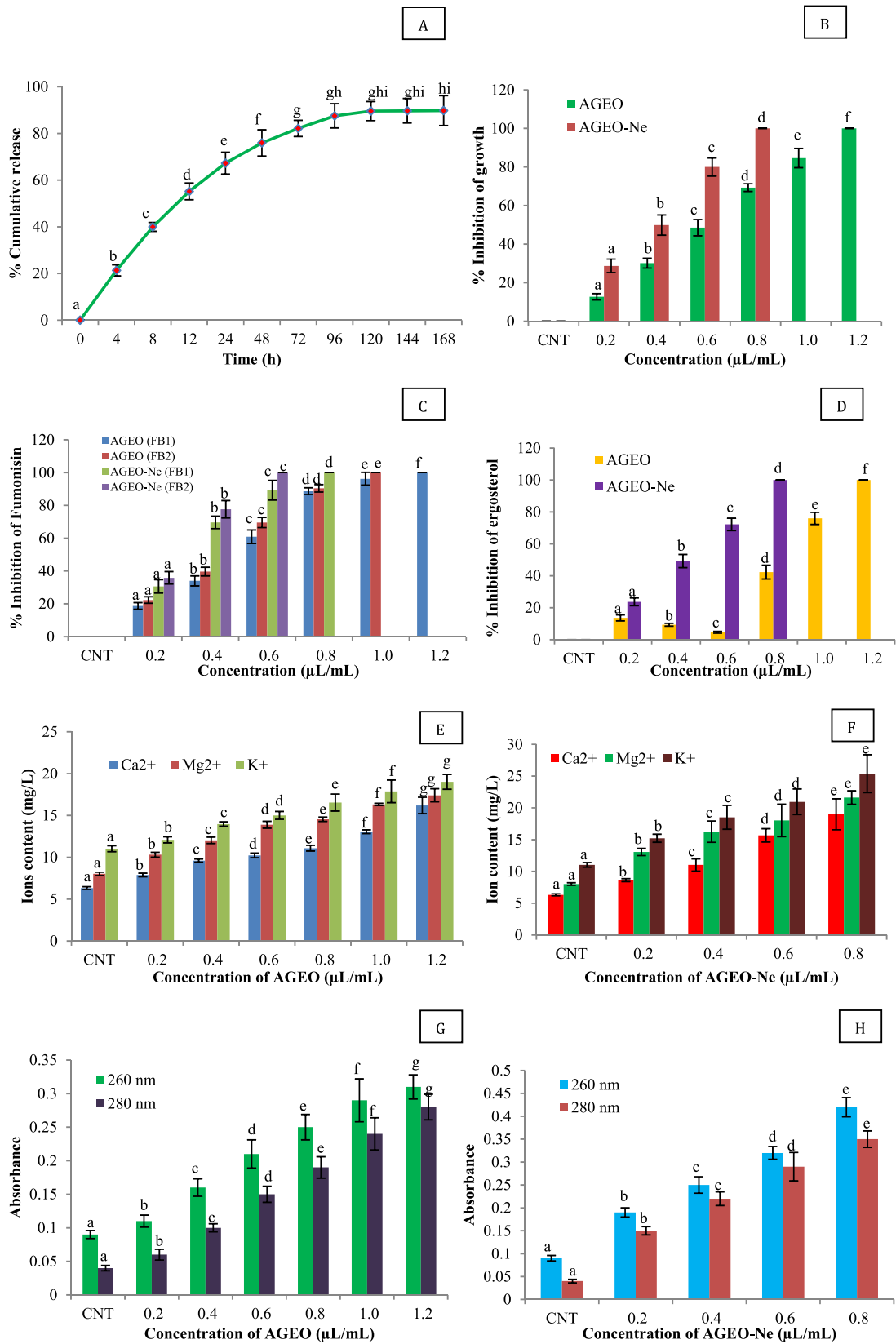
(caption on next page)

Fig. 2. (A) *In vitro* release of AGEO, (B) Effect of AGEO and AGEO-Ne against *F. verticill i oides* growth, (C) Effect of AGEO and AGEO-Ne against FB_1 and FB_2 production, (D) Effect of AGEO and AGEO-Ne against ergosterol production in *F. verticill i oides*, (E) Effect of AGEO on ions leakage from *F. verticill i oides* cells, (F) Effect of AGEO-Ne on ions leakage from *F. verticill i oides* cells, (G) Effect of AGEO on leakage of 260, 280 nm absorbing materials, (H) Effect of AGEO-Ne on leakage of 260, 280 nm absorbing materials. Values are mean (n = 3) ± SE; different letters represent significant differences at p value ≤ 0.05 according to ANOVA and Tukey's multiple comparison tests.

buffer saline (PBS) at pH 7.0 because the system simulates similar condition with majority of the stored food commodities. Most importantly, PBS is an isotonic solution which prevents the rupture and shriveling of cells and non-toxic in nature. Moreover, the pH of the stored rice samples was found in the range of 6.38–6.97 during mycoflora analysis (author's unpublished data). However, the change of pH of food commodities towards acidic one may lead to leaching of important dietary minerals and nutrients. Therefore, the release study was undertaken in PBS solution with neutral pH condition (pH 7). Nonetheless, lower pH may be opted for specific conditions where rapid release is desirable. The AGEO release prolife was characterized by two different phases. There was an initial burst phase release of 21.33 % in the beginning of the test after 4 h. The burst delivery has been explained by diffusion of AGEO from the surface layer of chitosan nanoparticles [62]. At (4–8) h and (8–12) h, the AGEO release was found to be 18.63 and 15.20 %, respectively. After 120 h, the AGEO discharge rate was comparatively slow which was due to the inefficacy of the buffer system to decimate the nanoparticles resulting very small discharge of oil [63]. A similar result on biphasic *in vitro* release of *Cinnamomum zeylanicum* essential oil from chitosan nanoparticles has been previously mentioned by Mohammadi et al. [64] which might be due to the weakening of electrostatic interaction between cationic chitosan with anionic S-TPP leading to quick and slow discharge periods. However, it is worth noting that the difference in release rate has been governed by the chemical structures of essential oils. The obtained result emphasized the controlled delivery of AGEO over a long term period which is an essential prerequisite of successful antimicrobial property in food system.

3.5. Antifungal and anti-fumonisin efficacy of AGEO and AGEO-Ne

The antifungal potency of AGEO against *F. verticill i oides* was measured in terms of minimum inhibitory concentration (MIC). At 0.2, 0.4, 0.6, 0.8, 1.0, and 1.2 µL/mL of AGEO the inhibition of *F. verticill i oides* growth was recorded to be 12.69, 30.14, 48.52, 69.30, 84.63, and 100 %, respectively (Fig. 2 B). Complete inhibition of FB_1 and FB_2 synthesis by AGEO was recognized at 1.2 and 1.0 µL/mL, respectively (Fig. 2C). For *in vitro* determination of FB_1 and FB_2 production, we have preferred thin layer chromatography (TLC) method because of increased amount of FB_1 and FB_2 produced by *F. verticill i oides* in *vitro* medium. Furthermore, it is also fast, less expensive, and widely used analytical method for mycotoxin quantification. The TLC method also requires comparatively lesser amount of organic solvents than high performance liquid chromatography (HPLC). Hence, in the present study TLC was used for *in vitro* determination of anti-fumonisin potential of AGEO and AGEO-Ne. However, for detection of FB_1 and FB_2 in stored rice seeds, HPLC method was used because FB_1 and FB_2 was present in quite small quantity that can't be quantified precisely by TLC. Our result displayed superior antifungal activity of AGEO over previously reported *Zingiber officinale* essential oil which inhibited *F. verticill i oides* growth at 2500 µg/mL [65]. The AGEO-Ne showed better inhibition of *F. verticill i oides* growth in a dose dependent fashion and complete inhibition of growth was recorded at 0.8 µL/mL (Fig. 2 B). However, 100 % inhibition of FB_1 and FB_2 biosynthesis by AGEO-Ne was observed at 0.8 and 0.6 µL/mL, respectively (Fig. 2C). Here, at the lower dose, FB_2 synthesis was completely checked as compared to the dose required for complete inhibition of FB_1 synthesis. This might be associated with the interaction of the essential oil and nanoformulation with the structural moiety of FB_1 and FB_2. Superior antifungal and anti-fumonisin efficacy of AGEO-Ne has been linked with nanometric size of particles having greater surface area to volume ratio.

3.6. Antifungal mode of action of AGEO and AGEO-Ne

Ergosterol is an important sterol of fungal plasma membrane that maintains the cellular growth, viability, integrity and membrane functionality [66,67]. Different antifungal agents have been reported to inhibit the cell growth by interrupting the synthesis of ergosterol. Therefore, determination of ergosterol content in *F. verticill i oides* by fumigation of AGEO and AGEO-Ne is considered to be an important parameter. The AGEO at 0.2, 0.4, and 0.6 µL/mL caused an oscillation for the synthesis of ergosterol which may be due to stress of the fungi during *in vitro* application of AGEO. The cell components in *F. verticill i oides* may activate some compensatory mechanisms for adaptive responses and reprogramming of gene expression for protection of cell membrane structure [68]. At 0.8, 1.0, and 1.2 µL/mL of AGEO, percent inhibition of ergosterol production was found to be 42.31, 75.96, and 100 %, respectively (Fig. 2 D). Disruption of lanosterol 14α-demethylase by essential oil may be a plausible basis for inhibition of ergosterol production in *F. verticill i oides* [69]. However, the greater inhibition of ergosterol content in *F. verticill i oides* cells with the values 23.67, 49.21, 72.19, and 100 % were recorded at 0.2, 0.4, 0.6, and 0.8 µL/mL doses of AGEO-Ne (Fig. 2 D). Better inhibitory activity against ergosterol biosynthesis has been associated with nanometric size of particles with greater surface area to volume ratio [70].

In the present study, the release of vital cellular contents like Ca^{2+}, Mg^{2+}, and K^+ ions from *F. verticill i oides* cells was significantly increased at different concentrations of AGEO over the control sets (Fig. 2 E). In the control set, the level of Ca^{2+}, Mg^{2+}, and K^+ ions was found to be 6.32, 8.02, and 11.03 mg/L, whereas, the *F. verticill i oides* cells treated with AGEO at 1.2 µL/mL showed maximum leakage of Ca^{2+}, Mg^{2+}, and K^+ ions with the values 16.20, 17.41, and 19.02 mg/L, respectively. The AGEO also caused significant efflux of nucleic acids (260 nm) and proteins (280 nm absorbing materials) from *F. verticill i oides* cells (Fig. 2 G). The optical density of 260 nm and 280 nm absorbing materials for the control set was recorded to be 0.09 and 0.04, respectively. However, the AGEO treated

(1.2 μL/mL) *F. verticilli oides* cells showed the optical density of 0.31 and 0.28 for 260 nm and 280 nm absorbing materials. The efflux of cellular constituents may lead to perturbation of metabolic functionalities, membrane transport, and disruption of cellular turgor pressure [71]. The hydrophobic activity of essential oil may damage the ergosterol synthesis along with increased efflux of cellular ions and eventually cause changes in membrane fluidity and cellular homoeostasis [72]. Moreover, the adverse effect on plasma membrane eventually led to perturbation of organelle activity, thereby causing cellular apoptosis. The AGEO-Ne at 0.8 μL/mL exhibited greater efflux of Ca^{2+}, Mg^{2+}, and K^+ ions with the values 18.99, 21.63, and 25.38 mg/L and 260 nm, 280 nm absorbing materials as compared to unencapsulated AGEO (Fig. 2 F, H). This greater efflux of ions has been related to sub-cellular size of particles with controlled delivery and targeted site of action.

### 3.7. Anti-fumonisin mechanism of action of AGEO: In silico investigation

In the present study, the molecular mechanism of anti-fumonisin activity was assessed through *in silico* interaction of linalyl acetate and geranyl acetate with FUM 21 protein. The FUM 21 is a Zn(II)2Cys6 DNA binding protein that help in transcriptional regulation and considered as a key protein of fumonisin biosynthesis pathway in *F. verticilli oides* [73]. The disruption of FUM 21 protein may block the fumonisin production. The *in silico* molecular binding was analyzed through global energy, attractive vander waal force and atomic contact energy. The energy indices have been widely used to characterize the molecular target site of ligand molecules to the receptor proteins [74]. In this research, the binding prediction was based on the minimum global binding energy of the ligand (linalyl acetate and geranyl acetate) and receptor (FUM 21 protein) bond. Different binding energies for interaction of linalyl acetate and geranyl acetate with FUM 21 protein is displayed in Table 3. The energy simulation suggested the establishment of possible hydrogen bonding interaction between the test compounds (linalyl acetate and geranyl acetate) and different amino acids viz., Ala 13, Val 15, Pro 88, Leu 654, Phe 655, Leu 658, and Glu 671 of FUM 21 proteins (Fig. 3A–C). This result was in line with the findings of Oufensou et al. [75], who also reported a frequent molecular interactions of monoterpenoids, phenylpropanoids, and phenylethanones with common sets of amino acids in trichodiene synthase (TRI5) that converts farnesyl pyrophosphate to trichodiene protein during *in silico* study. Hence, the results of this study demonstrated that the effective binding of linalyl acetate and geranyl acetate with FUM 21 protein may cause alteration in its stereo-spatial arrangements, leading to the inhibition of fumonisin biosynthesis.

3.8. Antioxidant activity of AGEO and AGEO-Ne

Oxidative stress in food commodities causes macromolecular damage manifesting the impairment of cellular function along with toxicity and disease symptoms. It has also been reported that FB_1 induces the synthesis of reactive oxygen species (ROS) in food commodities [76]. It has been noticed that several reaction in FB_1 pathways is mediated by oxygenase reactions [77]; therefore, high antioxidant activity dependent blockage of oxygenase action may be pointed out as a prime factor for inhibition of FB_1 biosynthesis in *F. verticilli oides* cells. Moreover, essential oil is a complex mixture of different terpenoids, sequiterpenoids, and phenolic components involving the synergistic reactive facets, hence the determination of antioxidant activity of AGEO and AGEO-Ne is of utmost important in the current study. Most notably, a single method is not able to justify the antioxidant capacity of essential oil, but at least two methods are required to ascertain the authenticity. To achieve this, the antioxidant activity of AGEO and AGEO-Ne was determined by two spectrophotometric methods like DPPH and ABTS assay. Different studies have also reported that antioxidant activity of essential oil is depended on phenolic constituents. Hence, besides evaluating the antioxidant activity total phenolic content measurement of AGEO and AGEO-Ne is an important parameter to be determined in the present piece of study. The total phenolic content of AGEO was measured to be 6.37 μg gallic acid equivalent/mg of oil, whereas entrapment slightly enhanced the phenolic content to 7.21 μg gallic acid equivalent/mg of oil which was evident from physical stabilization of AGEO phytochemical components in nanoemulsion system [78]. The radical quenching capability of AGEO and AGEO-Ne was measured through DPPH and ABTS assay. The antioxidant capacity was presented in terms of the IC_{50} values. The IC_{50} (half maximal inhibitory concentration) is defined as the concentration of the sample that can scavenge 50 % of free radicals. The IC_{50} value is inversely proportional to the DPPH and ABTS free radical scavenging activity or in other words we can say that the antioxidant property of AGEO and AGEO-Ne. This also means that less amounts of AGEO and AGEO-Ne are required to scavenge the free radicals if the IC_{50} value is less or vice versa. The AGEO IC_{50} value for DPPH and ABTS evaluation was recorded to be 20.17 and 9.56 μL/mL, respectively (Table 4). The AGEO-Ne showed better antioxidant activity with DPPH and ABTS IC_{50} values 12.08 and 6.40 μL/mL, respectively (Table 4). The CS-Ne showed very negligible antioxidant activity due to involvement of –NH_2 and –OH group in intramolecular hydrogen bonding in polymer chain cross-linking with S-TPP which prevent them from being unavailable for quenching of free radicals [61,79]. The higher antioxidant activity of AGEO-Ne over its unencapsulated form has been associated with better protection of phenolic components against oxygen [80]. Moreover, the sub-cellular

Table 3
Binding energy indices for interaction of linalyl acetate and geranyl acetate with FUM 21 protein.

Essential oil component	Receptor protein	Hydrogen bonding amino acids	Binding energy (Kcal/mol)		
			Global energy	Attractive Vander Waal force	Atomic contact energy
Linalyl acetate	FUM 21	Ala 13, Pro 88, Leu 654, Phe 655	−22.35	−13.35	−8.54
Geranyl acetate	FUM 21	Ala 13, Val 15, Pro 88, Leu 654, Phe 655, Leu 658, Glu 671, Leu 675	−26.37	−15.41	−10.32
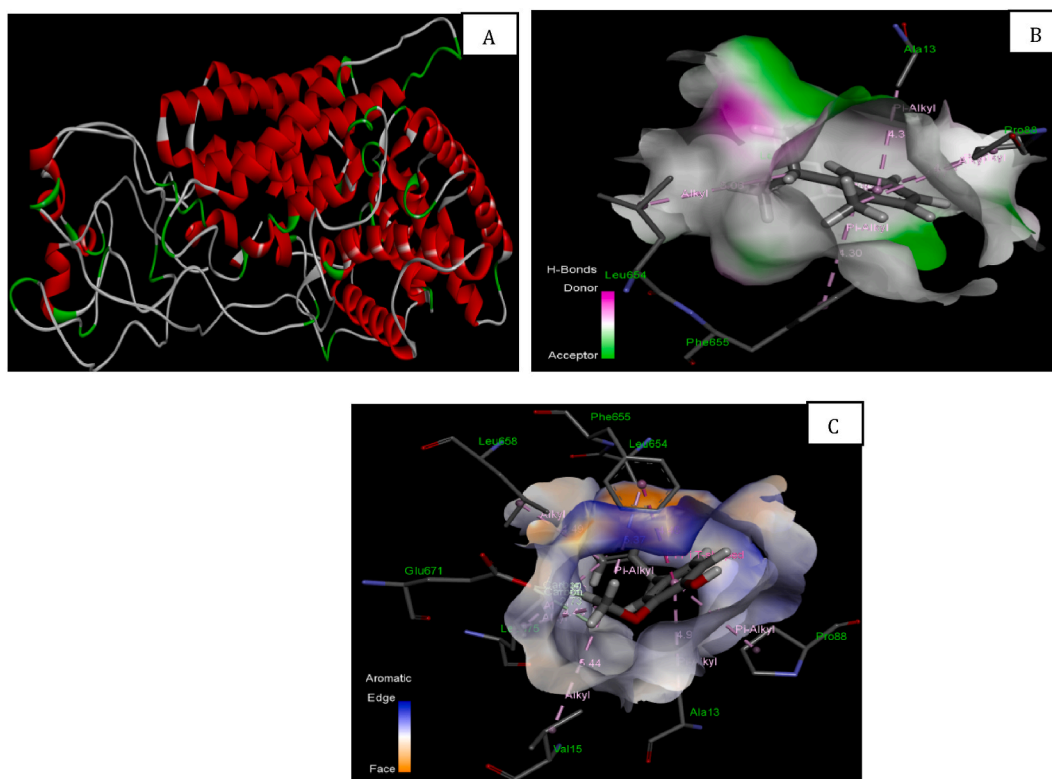
Fig. 3. (A) Three dimensional (3 D) structure of FUM 21 protein, (B) Interaction of linalyl acetate with FUM 21 protein, (C) Interaction of geranyl acetate with FUM 21 protein.

particle size with greater surface area and controlled release of AGEO has been ascribed for better inhibition of the free radical mediated chain reactions. The current result is coincided to Sindhu et al. [81] suggesting enhancement in free radical quenching capability of *Curcuma longa* essential oil when entrapped into chitosan nanobiopolymer. On the basis of the result the AGEO-Ne could be used as an excellent substitute to synthetic antioxidants for preservation of stored rice samples against fumonisin contamination and oxidative stress.

3.9. In situ antifungal and anti-fumonisin efficacy of AGEO and AGEO-Ne for protection of rice

The *in situ* efficacy assessment against *F. verticill i oides* contamination and FB_1, FB_2 biosynthesis in stored rice samples is an important parameter for field based application of AGEO and AGEO-Ne in agri-sectors. Most importantly, India is the major producer of rice and it is also exported to other countries on the basis of demands. Hence, cumulative attention has been paid for protection of rice against FB_1 and FB_2 contamination to maintain their content below the maximum toxic limit. In the present course of investigation, the *F. verticill i oides* count in uninoculated and inoculated rice samples was found to be 5.81 log cfu/g and 5.84 log cfu/g, respectively. However, the *F. verticill i oides* count for the AGEO fumigated uninoculated and inoculated rice samples (at 1.2 μL/mL dose) showed 4.95 log cfu/g and 5.07 log cfu/g, respectively. The AGEO fumigation at 1.2 μL/mL caused 82.09 % and 86.32 % protection against *F. verticill i oides* contamination in inoculated and uninoculated rice samples (Fig. 4 A). Complete inhibition of fungal proliferation was not achieved by AGEO treatment which might be linked with absorption of some volatile constituents by rice commodity itself. However, the AGEO-Ne fumigated rice samples did not show any *F. verticill i oides* colony and exhibited 100 %

Table 4
Antioxidant activity of AGEO and AGEO-Ne.

Essential oil/Nanoemulsion	DPPH IC$_{50}$ (μL/mL)	ABTS IC$_{50}$ (μL/mL)
AGEO	20.17 ± 2.03[a]	9.56 ± 2.00[a]
AGEO-Ne	12.08 ± 1.90[b]	6.40 ± 1.01[b]
CS-Ne	73.0 ± 4.52[c]	68.97 ± 5.41[c]

Note: Values are mean (n = 3) ± SE. The means followed by same letter in the same column are not significantly different according to ANOVA and Tukey's multiple comparison tests.
Absorbance of negative control for both assays was determined as 0 % inhibition.

protection against contamination in both inoculated and uninoculated treatment sets (Fig. 4 A). The inoculated and uninoculated control rice samples showed significant contamination of FB_1 and FB_2 content with 9.51, 7.98 and 8.26, 6.74 µg/kg, respectively (p ≤ 0.05). Most notably, both the AGEO and AGEO-Ne demonstrated 100 % inhibition of FB_1 and FB_2 biosynthesis in rice samples (Fig. 4 A). The complete inhibition of FB_1 and FB_2 biosynthesis in stored rice samples may also be attributed by promising antioxidant activity of essential oil [82]. Better antifungal and anti-fumonisin efficacy has been contributed by nano size of AGEO-Ne particles with greater surface to volume ratio and controlled delivery at the target site. Similar result has been reported by Singh et al. [24] exhibiting the
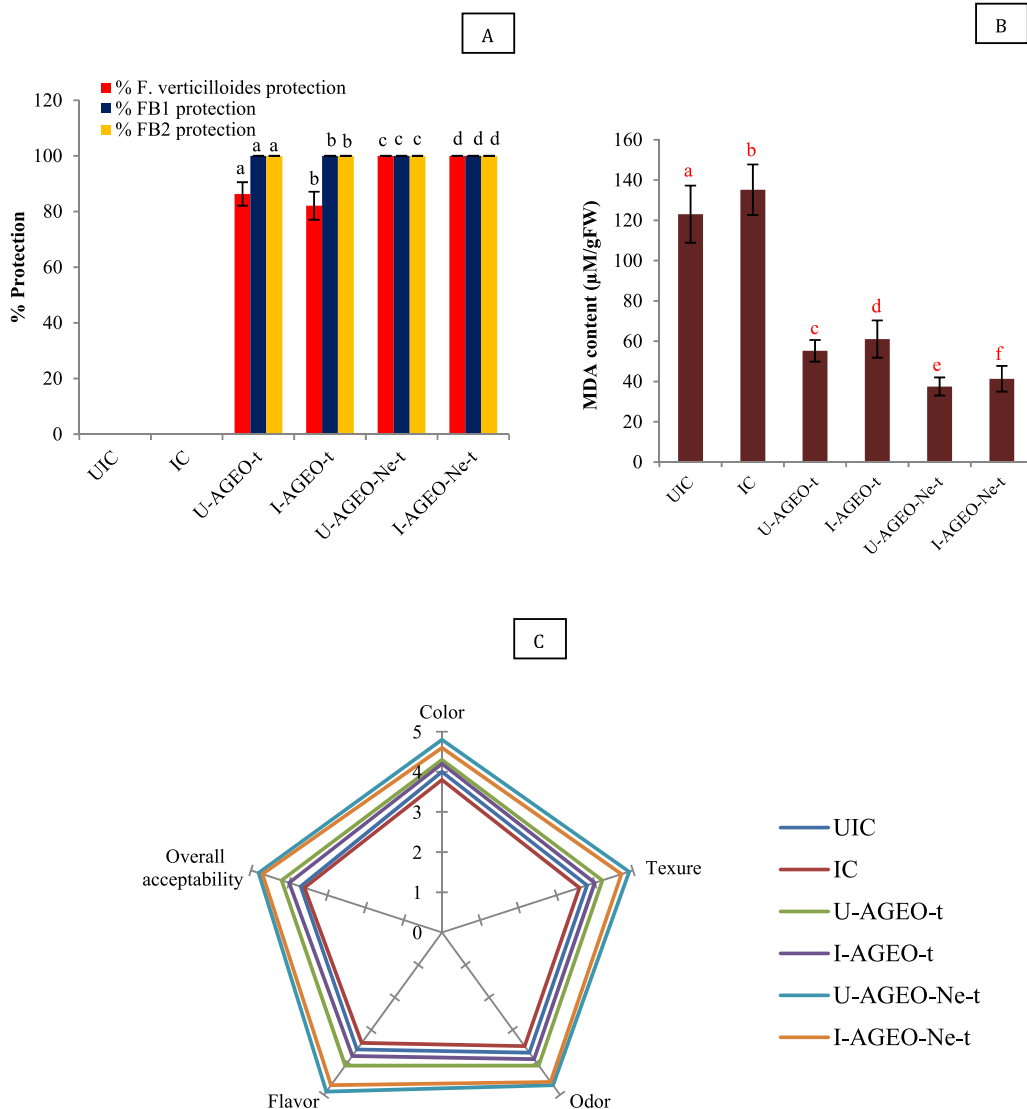
Note: **UIC** = Uninoculated control
IC = Inoculated control
U-AGEO-t = Uninoculated treatment with AGEO
I-AGEO-t = Inoculated treatment with AGEO
U-AGEO-Ne-t = Uninoculated treatment with AGEO-Ne
I-AGEO-Ne-t = Inoculated treatment with AGEO-Ne

Fig. 4. (A) *In situ* protection of rice samples by AGEO and AGEO-Ne against *F. verticill i oides*, FB_1 and FB_2 contamination, (B) Effect of AGEO and AGEO-Ne on lipid peroxidation of rice samples, (C) Effect of AGEO and AGEO-Ne on organoleptic profiles of rice samples. Values are mean (n = 3) ± SE; different letters represent significant differences at p value ≤ 0.05 according to ANOVA and Tukey's multiple comparison tests.

inhibition of fumonisin isolated from maize kernels by clove essential oil nanoemulsion. The antimycotoxigenic activity of essential oil and nanoformulations has also been associated with the inhibition of ROS production and detoxification/activation of biotransformation pathway, hence disrupting the signal transduction in mycotoxin synthesis [83]. Therefore, AGEO-Ne could be used as controlled and innovative delivery vehicle for inhibition of fumonisin mediated deterioration of stored rice samples.

3.10. Estimation of lipid peroxidation in rice

Lipid peroxidation is an indicator of oxidative deterioration of stored food samples by measuring the second stage autooxidation products, particularly malondialdehyde [84]. Moreover, the ROS also induce the catalysis of free radical mediated interaction of fatty acids with different food components resulting in the production of off-flavor and off-odor [85]. The lipid content in rice accounts for 0.2–1.0 %, but during storage the unsaturated fatty acids of rice are easily oxidized and decomposed developing free radical peroxides and other secondary oxidation products. The free radicals are potential initiating factors for chain polymerization in lipid and protein reaction system by hydrogen extraction. These lipid peroxides also affect the rice by reducing the edible quality and nutritional value [86]. The lipid free radicals also results in intramolecular and intermolecular cross-linking with protein which seriously cause loss in the availability of different amino acids like phenylalanine, lysine, tryptophan, tyrosine and methionine [87]. Moreover, the lipid peroxidation has also been associated with off-flavor and off-odor of rice during the storage periods. Hence, inhibition of lipid peroxidation by AGEO and its chitosan based nanoformulation is an important parameter to be considered to maintain the nutritional profile and edible quality of rice samples. The extent of lipid peroxidation depends on pH, oxygen concentration, fatty acid composition, ions distribution, and amount of lipid molecules present in foods [88]. In the current investigation, oxidation of rice lipids was measured through MDA and in the inoculated and uninoculated control set MDA content was recorded to be 135.21 and 123.06 μM/g FW, respectively (Fig. 4 B). However, the AGEO fumigated rice samples (inoculated and uninoculated sets) showed inhibition of lipid peroxidation and MDA content was found to be 61.08 and 55.23 μM/g FW. The lipid peroxidation inhibitory properties of AGEO might be associated with the presence of different compounds having promising free radical scavenging potentiality [89]. The AGEO-Ne fumigated rice samples at inoculated and uninoculated treatment showed reduction in MDA content with 41.35 and 37.52 μM/g FW, respectively. The superior efficacy of AGEO-Ne for inhibition of MDA biosynthesis may be associated with nanometric size of particles with greater surface to volume ratio and maximum free radical neutralizing capacity and better reaction kinetics for mitigation of terminal fatty acid oxidation. Our result showed similarity with the previous investigation of anethole loaded chitosan nanoemulsion for retardation of MDA content in stored maize samples [90]. However, our findings showed better efficacy of AGEO-Ne in mitigating MDA content which illustrated its superiority for promising application as nano-shelf life enhancer in agri-sectors.

3.11. Impact of AGEO and AGEO-Ne on organoleptic qualities of rice

Fig. 4C presents effects of AGEO and AGEO-Ne on color, flavor, odor, and texture of different rice samples. The changes of color and texture in control and fumigated rice samples were not as obvious as odor and flavor. The flavor and odor score of control rice samples was 3.4 and 3.5, respectively which was found significantly lower than the AGEO and AGEO-Ne fumigated rice samples. In case of AGEO fumigated rice samples, somewhat aromatic smell was achieved whereas the AGEO-Ne fumigated rice samples showed significant protection of all the organoleptic attributes. The possible reason for unfavorable odor and flavor in control rice samples has been associated with fungal spoilage, FB$_1$ and FB$_2$ production, and lipid peroxidation [91]. The improvement of organoleptic qualities in rice samples by AGEO-Ne treatment has been associated with the sustained delivery of essential oil from chitosan nanoemulsion [42]. The above result confirmed the application of AGEO-Ne for preservation of organoleptic attributes of food commodities in agri-sectors.

4. Conclusion

Nanoencapsulation of AGEO into chitosan matrix improved the antifungal and anti-fumonisin efficacy in stored rice samples. The controlled delivery of AGEO facilitated the long term protection of rice samples against *F. verticill i oides* and FB$_1$, FB$_2$ contamination. The exploration of ergosterol impairment and release of cell contents confirmed plasma membrane as a plausible target of antifungal action. The interaction of AGEO components with FUM 21 protein validated the anti-fumonisin mechanism of action. The AGEO-Ne showed prominent *in situ* antifungal, anti-fumonisin efficacy and lipid peroxidation inhibitory potency in rice samples without altering the organoleptic attributes. In view of the above results, the AGEO-Ne nanoemulsion may be used as a novel nano-green preservative in food based agricultural sectors. Moreover, as a future perspective additional data is necessary for the full elucidation of the mechanism of action and the molecular basis of the inhibition of fumonisin synthesis would be explored for large scale commercial application.

Data availability statement

Data will be made available on request.

Ethical statement

Additional information

No additional information is available for this paper.

CRediT authorship contribution statement

Somenath Das: Writing – review & editing, Writing – original draft, Visualization, Validation, Supervision, Software, Methodology, Investigation, Formal analysis, Data curation, Conceptualization. **Anand Kumar Chaudhari:** Methodology, Formal analysis, Data curation.

Declaration of competing interest

The authors declare that they have no known competing financial interests or personal relationships that could have appeared to influence the work reported in this paper.

Acknowledgments

References

[1] K.A. Voss, G.W. Smith, W.M. Haschek, Fumonisins: Toxicokinetics, mechanism of action and toxicity, Anim. Feed Sci. Technol. 137 (2007) 299–325, https://doi.org/10.1016/j.anifeedsci.2007.06.007.

[2] J.P. Rheeder, W.F. Marasas, H.F. Vismer, Production of fumonisin analogs by *Fusarium* species, Appl. Environ. Microbiol. 68 (2002) 2101–2105, https://doi.org/10.1128/AEM.68.5.2101-2105.2002.

[3] F. Ahangarkani, S. Rouhi, I. Gholamour Azizi, A review on incidence and toxicity of fumonisins, Toxin Rev. 33 (2014) 95–100, https://doi.org/10.3109/15569543.2013.871563.

[4] IARC (International Agency for Research on Cancer) Some traditional herbal medicines, some mycotoxins, Naphthalene and Styrene, vol. 82, IARC, Lyon, France, 2002, pp. 301–366.

[5] R.N. Wangia-Dixon, K. Nishimwe, Molecular toxicology and carcinogenesis of fumonisins: a review, J. Environ. Sci. Health C 39 (2020) 44–67, https://doi.org/10.1080/26896583.2020.1867449.

[6] P.N. Achar, M.Y. Sreenivasa, Current perspectives of biocontrol agents for management of Fusarium verticillioides and its fumonisin in cereals—a review, J Fungus 7 (2021) 776–789, https://doi.org/10.3390/jof7090776.

[7] S. Das, A.K. Chaudhari, A review on the efficacy of essential oils and their nanoencapsulated formulations against aflatoxins contamination of major cereals with emphasis on mode of action, Biocatal. Agric. Biotechnol. 53 (2023) 102861, https://doi.org/10.1016/j.bcab.2023.102861.

[8] S. Das, V.K. Singh, A.K. Dwivedy, A.K. Chaudhari, N.K. Dubey, Insecticidal and fungicidal efficacy of essential oils and nanoencapsulation approaches for the development of next generation ecofriendly green preservers for management of stored food commodities: an overview, Int. J. Pest Manag. (2021) 1–32, https://doi.org/10.1080/09670874.2021.1969473.

[9] S. Basak, P. Guha, A review on antifungal activity and mode of action of essential oils and their delivery as nano-sized oil droplets in food system, J. Food Sci. Technol. 55 (2018) 4701–4710, https://doi.org/10.1007/s13197-018-3394-5.

[10] A.S. Doost, M.N. Nasrabadi, V. Kassozi, H. Nakisozi, P. Van der Meeren, Recent advances in food colloidal delivery systems for essential oils and their main components, Trends Food Sci. Technol. 99 (2020) 474–486, https://doi.org/10.1016/j.tifs.2020.03.037.

[11] R. Karami-Osboo, M. Mahboubifar, M. Mirabolfathy, L. Hosseinian, A.R. Jassbi, Encapsulated *Zataria multiflora*'s essential oil inhibited the growth of *Aspergillus flavus* and reduced aflatoxins levels in contaminated pistachio nut, Biocatal. Agric. Biotechnol. 51 (2023) 1–9, https://doi.org/10.1016/j.bcab.2023.102796.

[12] A.B. Roshan, H.N. Venkatesh, N.K. Dubey, D.C. Mohana, Chitosan-based nanoencapsulation of *Toddalia asiatica* (L.) Lam. essential oil to enhance antifungal and aflatoxin B_1 inhibitory activities for safe storage of maize, Int. J. Biol. Macromol. 204 (2022) 476–484, https://doi.org/10.1016/j.ijbiomac.2022.02.026.

[13] N.K. Kalagatur, O.S. Nirmal Ghosh, N. Sundararaj, V. Mudili, Antifungal activity of chitosan nanoparticles encapsulated with *Cymbopogon martinii* essential oil on plant pathogenic fungi *Fusarium graminearum*, Front. Pharmacol. 9 (2018) 1–13, https://doi.org/10.3389/fphar.2018.00610.

[14] S. Das, V.K. Singh, A.K. Dwivedy, A.K. Chaudhari, N.K. Dubey, *Anethum graveolens* essential oil encapsulation in chitosan nanomatrix: investigations on *in vitro* release behavior, organoleptic attributes, and efficacy as potential delivery vehicles against biodeterioration of rice (*Oryza sativa* L.), Food Bioprocess Technol. 14 (2021) 831–853, https://doi.org/10.1007/s11947-021-02589-z.

[15] A.K. Pandey, P. Kumar, P. Singh, N.N. Tripathi, V.K. Bajpai, Essential oils: Sources of antimicrobials and food preservatives, Future Microbiol. 7 (2017) 2161–2169, https://doi.org/10.3389/fmicb.2016.02161.

[16] B. Salehi, A. Venditti, C. Frezza, A. Yücetepe, Ü. Altuntaş, S. Uluata, J. Sharifi-Rad, Apium plants: beyond simple food and pharmacological applications, Appl. Sci. 9 (2019) 3547–3568, https://doi.org/10.3390/app9173547.

[17] A. Kedia, A.K. Dwivedy, D.K. Jha, N.K. Dubey, Efficacy of *Mentha spicata* essential oil in suppression of *Aspergillus flavus* and aflatoxin contamination in chickpea with particular emphasis to mode of antifungal action, Protoplasma 253 (2016) 647–653, https://doi.org/10.1007/s00709-015-0871-9.

[18] S. Das, V.K. Singh, A.K. Dwivedy, A.K. Chaudhari, N.K. Dubey, Exploration of some potential bioactive essential oil components as green food preservative, LWT–Food Sci. Technol. 137 (2021) 1–8, https://doi.org/10.1016/j.lwt.2020.110498.

[19] R.P. Adams, Identification of Essential Oil Components by Gas Chromatography/mass Spectrometry, 5 online ed., Texensis Publishing, TX USA, 2017. Gruver.

[20] S.F. Hosseini, M. Zandi, M. Rezaei, F. Farahmandghavi, Two-step method for encapsulation of oregano essential oil in chitosan nanoparticles: preparation, characterization and in vitro release study, Carbohydr. Polym. 95 (2013) 50–56, https://doi.org/10.1016/j.carbpol.2013.02.031.

[21] S. Das, A.K. Chaudhari, V.K. Singh, B.K. Singh, N.K. Dubey, High speed homogenization assisted encapsulation of synergistic essential oils formulation: characterization, *in vitro* release study, safety profile, and efficacy towards mitigation of aflatoxin B$_1$ induced deterioration in rice samples, Food Chem. Toxicol. 169 (2022) 113443, https://doi.org/10.1016/j.fct.2022.113443.

[22] L.O. Xavier, W.G. Sganzerla, G.B. Rosa, C.G. da Rosa, L. Agostinetto, A.P. de Lima Veeck, M.R. Nunes, Chitosan packaging functionalized with *Cinnamodendron dinisii* essential oil loaded zein: a proposal for meat conservation, Int. J. Biol. Macromol. 169 (2021) 183–193, https://doi.org/10.1016/j.ijbiomac.2020.12.093.

[23] A. Esmaeili, A. Asgari, *In vitro* release and biological activities of *Carum copticum* essential oil (CEO) loaded chitosan nanoparticles, Int. J. Biol. Macromol. 81 (2015) 283–290, https://doi.org/10.1016/j.ijbiomac.2015.08.010.

[24] P. Singh, N. Dasgupta, V. Singh, N.C. Mishra, H. Singh, S.D. Purohit, B.N. Mishra, Inhibitory effect of clove oil nanoemulsion on fumonisin isolated from maize kernels, LWT–Food Sci. Technol. 134 (2020) 110237, https://doi.org/10.1016/j.lwt.2020.110237.

[25] M.B. Aboul-Nasr, M.R.A. Obied-Allah, Biological and chemical detection of fumonisins produced on agar medium by *Fusarium verticillioides* isolates collected from corn in Sohag, Egypt, Microbiol. 159 (2013) 1720–1724, https://doi.org/10.1099/mic.0.069039-0.

[26] L.M. Sun, K. Liao, S. Liang, P.H. Yu, D.Y. Wang, Synergistic activity of magnolol with azoles and its possible antifungal mechanism against *Candida albicans*, J. Appl. Microbiol. 118 (2015) 826–838, https://doi.org/10.1111/jam.12737.

[27] A.K. Dwivedy, B. Prakash, C.S. Chanotiya, D. Bisht, N.K. Dubey, Chemically characterized *Mentha cardiaca* L. essential oil as plant based preservative in view of efficacy against biodeteriorating fungi of dry fruits, aflatoxin secretion, lipid peroxidation and safety profile assessment, Food Chem. Toxicol. 106 (2017) 175–184, https://doi.org/10.1016/j.fct.2017.05.043.

[28] A.K. Chaudhari, V.K. Singh, S. Das, J. Prasad, A.K. Dwivedy, N.K. Dubey, Improvement of in vitro and in situ antifungal, AFB$_1$ inhibitory and antioxidant activity of *Origanum majorana* L. essential oil through nanoemulsion and recommending as novel food preservative, Food Chem. Toxicol. 143 (2020) 111536, https://doi.org/10.1016/j.fct.2020.111536.

[29] S. Das, A.K. Chaudhari, V.K. Singh, A.K. Dwivedy, N.K. Dubey, Encapsulation of carvone in chitosan nanoemulsion as edible film for preservation of slice breads against *Aspergillus flavus* contamination and aflatoxin B$_1$ production, Food Chem. 430 (2024) 137038, https://doi.org/10.1016/j.foodchem.2023.137038.

[30] R. Re, N. Pellegrini, A. Proteggente, A. Pannala, M. Yang, C. Rice-Evans, Antioxidant activity applying an improved ABTS radical cation decolorization assay, Free Radic. Biol. Med. 26 (1999) 1231–1237, https://doi.org/10.1016/S0891-5849(98)00315-3.

[31] M.B. Gholivand, M. Rahimi-Nasrabadi, H. Batooli, A.H. Ebrahimabadi, Chemical composition and antioxidant activities of the essential oil and methanol extracts of *Psammogeton canescens*, Food Chem. Toxicol. 48 (2010) 24–28, https://doi.org/10.1016/j.fct.2009.09.007.

[32] P.K. Mishra, B. Prakash, A. Kedia, A.K. Dwivedy, N.K. Dubey, S. Ahmad, Efficacy of *Caesulia axillaris, Cymbopogon khasans* and *Cymbopogon martinii* essential oils as plant based preservatives against degradation of raw materials of *Andrographis paniculata* by fungal spoilage, Int. Biodeterior. Biodegrad. 104 (2015) 244–250, https://doi.org/10.1016/j.ibiod.2015.06.015.

[33] A. Visconti, M. Solfrizzo, A.D. Girolamo, Collaborators: Bresch H Burdaspal P Castegnaro M Felgueiras I Gardikis J Jørgensen K Kakouri; E Kretschmer H Lew H Meyer K Miller J Møller T Nuotio K Patel S Pietri A Pittet A Sizoo E Spanjer; MC Steiner W Tiebach R Usleber E C von Holst P. Wilson, Determination of fumonisins B$_1$ and B$_2$ in corn and corn flakes by liquid chromatography with immunoaffinity column cleanup: collaborative study, J. AOAC Int. 84 (2001) 1828–1838, https://doi.org/10.1093/jaoac/84.6.1828.

[35] S. Das, V.K. Singh, A.K. Chaudhari, A.K. Dwivedy, N.K. Dubey, Fabrication, physico-chemical characterization, and bioactivity evaluation of chitosan-linalool composite nano-matrix as innovative controlled release delivery system for food preservation, Int. J. Biol. Macromol. 188 (2021) 751–763, https://doi.org/10.1016/j.ijbiomac.2021.08.045.

[36] I. Clemente, M. Aznar, C. Nerín, Synergistic properties of mustard and cinnamon essential oils for the inactivation of food borne moulds *in vitro* and on Spanish bread, Int. J. Food Microbiol. 298 (2019) 44–50, https://doi.org/10.1016/j.ijfoodmicro.2019.03.012.

[37] S. Das, V.K. Singh, A.K. Dwivedy, A.K. Chaudhari, N. Upadhyay, A. Singh, N.K. Dubey, Antimicrobial activity, antiaflatoxigenic potential and *in situ* efficacy of novel formulation comprising of *Apium graveolens* essential oil and its major component, Pestic. Biochem. Physiol. 160 (2019) 102–111, https://doi.org/10.1016/j.pestbp.2019.07.013.

[38] J.A. Dąbrowska, A. Kunicka-Styczyńska, K.B. Śmigielski, Biological, chemical, and aroma profiles of essential oil from waste celery seeds (*Apium graveolens* L.), J. Essent. Oil Res. 32 (2020) 308–315, https://doi.org/10.1080/10412905.2020.1754937.

[39] N.H. Hassanen, A.M.F. Eissa, S.A.M. Hafez, E.A. Mosa, Antioxidant and antimicrobial activity of celery (*Apium graveolens*) and coriander (*Coriandrum sativum*) herb and seed essential oils, Int. J. Curr. Microbiol. App. Sci. 4 (2015) 284–296.

[40] E. Rozek, R. Nurzynska-Wierdak, A. Salata, P. Gumiela, The chemical composition of the essential oil of leaf celery (*Apium graveolens* L. var. *Secalinum* Alef.) under the plants' irrigation and harvesting method, Acta Sci. Pol. 15 (2016) 149–159.

[41] S.M.B. Hashemi, A.M. Khaneghah, M.G. Ghahfarrokhi, I. Eş, Basil-seed gum containing *Origanum vulgare* subsp. viride essential oil as edible coating for fresh cut apricots, Postharvest Biol. Technol. 125 (2017) 26–34, https://doi.org/10.1016/j.postharvbio.2016.11.003.

[42] A.K. Chaudhari, V.K. Singh, S. Das, N.K. Dubey, Fabrication, characterization, and bioactivity assessment of chitosan nanoemulsion containing allspice essential oil to mitigate *Aspergillus flavus* contamination and aflatoxin B$_1$ production in maize, Food Chem. 372 (2022) 131221, https://doi.org/10.1016/j.foodchem.2021.131221.

[43] E.J.D. de Souza, D.H. Kringel, A.R.G. Dias, E. da Rosa Zavareze, Polysaccharides as wall material for the encapsulation of essential oils by electrospun technique, Carbohydr. Polym. 265 (2021) 118068, https://doi.org/10.1016/j.carbpol.2021.118068.

[44] S. Das, V.K. Singh, A.K. Dwivedy, A.K. Chaudhari, N.K. Dubey, Nanostructured *Pimpinella anisum* essential oil as novel green food preservative against fungal infestation, aflatoxin B$_1$ contamination and deterioration of nutritional qualities, Food Chem. 344 (2021) 128574, https://doi.org/10.1016/j.foodchem.2020.128574.

[45] S.M. Jafari, E. Assadpoor, Y. He, B. Bhandari, Encapsulation efficiency of food flavours and oils during spray drying, Dry. Technol. 26 (2008) 816–835, https://doi.org/10.1080/07373930802135972.

[46] G.W. Padua, Q. Wang, Controlled self-organization of zein nanostructures for encapsulation of food ingredients in Micro/Nanoencapsulation of Active Food Ingredients (2009) 143–156, https://doi.org/10.1021/bk-2009-1007.ch009.

[47] K.A. Omar, L. Shan, X. Zou, Z. Song, X. Wang, Effects of two emulsifiers on yield and storage of flaxseed oil powder by response surface methodology, Pakistan J. Nutr. 8 (2009) 1316–1324.

[48] S. Hasani, S.M. Ojagh, M. Ghorbani, Nanoencapsulation of lemon essential oil in Chitosan-Hicap system. Part 1: study on its physical and structural characteristics, Int. J. Biol. Macromol. 115 (2018) 143–151, https://doi.org/10.1016/j.ijbiomac.2018.04.038.

[49] S. Gupta, P.S. Variyar, Nanoencapsulation of essential oils for sustained release: application as therapeutics and antimicrobials, in: Encapsulations, Academic Press, 2016, pp. 641–672.

[50] C. Maes, S. Bouquillon, M.L. Fauconnier, Encapsulation of essential oils for the development of biosourced pesticides with controlled release: a review, Molecules 24 (2019) 1–15, https://doi.org/10.3390/molecules24142539.

[51] M. Hadidi, S. Pouramin, F. Adinepour, S. Haghani, S.M. Jafari, Chitosan nanoparticles loaded with clove essential oil: characterization, antioxidant and antibacterial activities, Carbohydr. Polym. 236 (2020) 116075, https://doi.org/10.1016/j.carbpol.2020.116075.

[52] A.K. Chaudhari, V.K. Singh, S. Das, N.K. Dubey, Nanoencapsulation of essential oils and their bioactive constituents: a novel strategy to control mycotoxin contamination in food system, Food Chem. Toxicol. 149 (2021) 112019, https://doi.org/10.1016/j.fct.2021.112019.

[53] G. Arya, M. Vandana, S. Acharya, S.K. Sahoo, Enhanced antiproliferative activity of Herceptin (HER2)-conjugated gemcitabine-loaded chitosan nanoparticle in pancreatic cancer therapy, Nanomed. Nanotechnol. Biol. Med. 7 (2011) 859–870, https://doi.org/10.1016/j.nano.2011.03.009.

[54] L. Keawchaoon, R. Yoksan, Preparation, characterization and in vitro release study of carvacrol-loaded chitosan nanoparticles, Colloids Surf., B 84 (2011) 163–171, https://doi.org/10.1016/j.colsurfb.2010.12.031.

[55] M. Hasani, A.E. Rad, M.M. Hosseini, M.S. Noghabi, Physicochemical characteristic of microencapsulated fish oil by freeze-drying using different combinations of wall materials, Biosci. Biotechnol. Res. Asia 12 (2015) 45–51.

[56] S. Woranuch, R. Yoksan, Eugenol-loaded chitosan nanoparticles: I. Thermal stability improvement of eugenol through encapsulation, Carbohydr. Polym. 96 (2013) 578–585, https://doi.org/10.1016/j.carbpol.2012.08.117.

[57] M. Mondéjar-López, A. Rubio-Moraga, A.J. López-Jimenez, J.C.G. Martínez, O. Ahrazem, L. Gómez-Gómez, E. Niza, Chitosan nanoparticles loaded with garlic essential oil: a new alternative to tebuconazole as seed dressing agent, Carbohydr. Polym. 277 (2022) 118815, https://doi.org/10.1016/j.carbpol.2021.118815.

[58] S. Das, A.K. Chaudhari, V.K. Singh, A.K. Dwivedy, N.K. Dubey, Angelica archangelica essential oil loaded chitosan nanoemulsion as edible coating for preservation of table grape fruit against Botrytis cinerea contamination and storage quality deterioration, Postharvest Biol. Technol. 205 (2023) 112482, https://doi.org/10.1016/j.postharvbio.2023.112482.

[59] M. Cai, Y. Wang, R. Wang, M. Li, W. Zhang, J. Yu, R. Hua, Antibacterial and antibiofilm activities of chitosan nanoparticles loaded with *Ocimum basilicum* L. essential oil, Int. J. Biol. Macromol. 202 (2022) 122–129, https://doi.org/10.1016/j.ijbiomac.2022.01.066.

[60] D. Kavaz, M. Idris, C. Onyebuchi, Physiochemical characterization, antioxidative, anticancer cells proliferation and food pathogens antibacterial activity of chitosan nanoparticles loaded with *Cyperus articulatus* rhizome essential oils, Int. J. Biol. Macromol. 123 (2019) 837–845, https://doi.org/10.1016/j.ijbiomac.2018.11.177.

[61] A. Shetta, J. Kegere, W. Mamdouh, Comparative study of encapsulated peppermint and green tea essential oils in chitosan nanoparticles: encapsulation, thermal stability, in-vitro release, antioxidant and antibacterial activities, Int. J. Biol. Macromol. 126 (2019) 731–742, https://doi.org/10.1016/j.ijbiomac.2018.12.161.

[62] M. Soltanzadeh, S.H. Peighambardoust, B. Ghanbarzadeh, M. Mohammadi, J.M. Lorenzo, Chitosan nanoparticles encapsulating lemongrass (*Cymbopogon commutatus*) essential oil: Physicochemical, structural, antimicrobial and in-vitro release properties, Int. J. Biol. Macromol. 192 (2021) 1084–1097, https://doi.org/10.1016/j.ijbiomac.2021.10.070.

[63] S.A. Agnihotri, N.N. Mallikarjuna, T.M. Aminabhavi, Recent advances on chitosan-based micro-and nanoparticles in drug delivery, J. Contr. Release 100 (2004) 5–28, https://doi.org/10.1016/j.jconrel.2004.08.010.

[64] A. Mohammadi, S.M. Hosseini, M. Hashemi, Emerging chitosan nanoparticles loading-system boosted the antibacterial activity of *Cinnamomum zeylanicum* essential oil, Ind. Crop. Prod. 155 (2020) 112824, https://doi.org/10.1016/j.indcrop.2020.112824.

[65] M.M.G. Yamamoto-Ribeiro, R. Grespan, C.Y. Kohiyama, F.D. Ferreira, S.A.G. Mossini, E.L. Silva, M.M. Junior, Effect of *Zingiber officinale* essential oil on *Fusarium verticillioides* and fumonisin production, Food Chem. 141 (2013) 3147–3152, https://doi.org/10.1016/j.foodchem.2013.05.144.

[66] J. Wei, Y. Bi, H. Xue, Y. Wang, Y. Zong, D. Prusky, Antifungal activity of cinnamaldehyde against *Fusarium sambucinum* involves inhibition of ergosterol biosynthesis, J. Appl. Microbiol. 129 (2020) 256–265, https://doi.org/10.1111/jam.14601.

[67] S. Das, Efficacy of *Pinus roxburghii* Sarg. essential oil against *Fusarium proliferatum* and fumonisin contamination in stored rice samples, Nat. Prod. Res. (2023) 1–5, https://doi.org/10.1080/14786419.2023.2294110.

[68] M. Parveen, M.K. Hasan, J. Takahashi, Y. Murata, E. Kitagawa, O. Kodama, H. Iwahashi, Response of *Saccharomyces cerevisiae* to a monoterpene: evaluation of antifungal potential by DNA microarray analysis, J. Antimicrob. Chemother. 54 (2004) 46–55, https://doi.org/10.1093/jac/dkh245.

[69] X. Sun, W. Wang, K. Wang, X. Yu, J. Liu, F. Zhou, S. Li, Sterol C-22 desaturase ERG5 mediates the sensitivity to antifungal azoles in *Neurospora crassa* and *Fusarium verticillioides*, Future Microbiol. 4 (2013) 127–134, https://doi.org/10.3389/fmicb.2013.00127.

[70] V.K. Singh, S. Das, A.K. Dwivedy, R. Rathore, N.K. Dubey, Assessment of chemically characterized nanoencapuslated *Ocimum sanctum* essential oil against aflatoxigenic fungi contaminating herbal raw materials and its novel mode of action as methyglyoxal inhibitor, Postharvest Biol. Technol. 153 (2019) 87–95, https://doi.org/10.1016/j.postharvbio.2019.03.022.

[71] Y. Zhang, X. Liu, Y. Wang, P. Jiang, S. Quek, Antibacterial activity and mechanism of cinnamon essential oil against *Escherichia coli* and *Staphylococcus aureus*, Food Control 59 (2016) 282–289, https://doi.org/10.1016/j.foodcont.2015.05.032.

[72] T. Hou, S.S. Sana, H. Li, Y. Xing, A. Nanda, V.R. Netala, Z. Zhang, Essential oils and its antibacterial, antifungal and anti-oxidant activity applications: a review, Food Biosci. 47 (2022) 101716, https://doi.org/10.1016/j.fbio.2022.101716.

[73] T. Li, X. Su, H. Qu, X. Duan, Y. Jiang, Biosynthesis, regulation, and biological significance of fumonisins in fungi: current status and prospects, Crit. Rev. Microbiol. 48 (2022) 450–462, https://doi.org/10.1080/1040841X.2021.1979465.

[74] A. Kumar, A. Kujur, A. Yadav, S. Pratap, B. Prakash, Optimization and mechanistic investigations on antifungal and aflatoxin B_1 inhibitory potential of nanoencapsulated plant-based bioactive compounds, Ind. Crop. Prod. 131 (2019) 213–223, https://doi.org/10.1016/j.indcrop.2019.01.043.

[75] S. Oufensou, A. Dessì, R. Dallocchio, V. Balmas, E. Azara, P. Carta, G. Delogu, Molecular docking and comparative inhibitory efficacy of naturally occurring compounds on vegetative growth and deoxynivalenol biosynthesis in *Fusarium culmorum*, Toxins 13 (2021) 759–765, https://doi.org/10.3390/toxins13110759.

[76] T. Arumugam, T. Ghazi, N.S. Abdul, A.A. Chuturgoon, A review on the oxidative effects of the fusariotoxins: fumonisin B_1 and fusaric acid, Toxicology in Oxidative Stress and Dietary Antioxidants (2021) 181–190, https://doi.org/10.1016/B978-0-12-819092-0.00019-4.

[77] J.A. Seo, R.H. Proctor, R.D. Plattner, Characterization of four clustered and coregulated genes associated with fumonisin biosynthesis in *Fusarium verticillioides*, Fungal Genet. Biol. 34 (2001) 155–165, https://doi.org/10.1006/fgbi.2001.1299.

[78] A.M. Pisoschi, A. Pop, C. Cimpeanu, V. Turcuş, G. Predoi, F. Iordache, Nanoencapsulation techniques for compounds and products with antioxidant and antimicrobial activity-A critical view, Eur. J. Med. Chem. 157 (2018) 1326–1345, https://doi.org/10.1016/j.ejmech.2018.08.076.

[79] S. Das, V.K. Singh, A.K. Chaudhari, A.K. Dwivedy, N.K. Dubey, Co-encapsulation of *Pimpinella anisum* and *Coriandrum sativum* essential oils based synergistic formulation through binary mixture: physico-chemical characterization, appraisal of antifungal mechanism of action, and application as natural food preservative, Pestic. Biochem. Physiol. 184 (2022) 105066, https://doi.org/10.1016/j.pestbp.2022.105066.

[80] B. Vafania, M. Fathi, S. Soleimanian-Zad, Nanoencapsulation of thyme essential oil in chitosan-gelatin nanofibers by nozzle-less electrospinning and their application to reduce nitrite in sausages, Food Bioprod. Process. 116 (2019) 240–248, https://doi.org/10.1016/j.fbp.2019.06.001.

[81] M. Sindhu, V. Rajkumar, C.A. Annapoorani, C. Gunasekaran, M. Kannan, Nanoencapsulation of garlic essential oil using chitosan nanopolymer and its antifungal and anti-aflatoxin B_1 efficacy in vitro and in situ, Int. J. Biol. Macromol. 243 (2023) 125160, https://doi.org/10.1016/j.ijbiomac.2023.125160.

[82] J.S. Dambolena, M.P. Zunino, A.G. López, H.R. Rubinstein, J.A. Zygadlo, J.W. Mwangi, S.T. Kariuki, Essential oils composition of *Ocimum basilicum* L. and *Ocimum gratissimum* L. from Kenya and their inhibitory effects on growth and fumonisin production by *Fusarium verticillioides*, Innovat. Food Sci. Emerg. Technol. 11 (2010) 410–414, https://doi.org/10.1016/j.ifset.2009.08.005.

[83] L. Pinto, M.R. Tapia-Rodríguez, F. Baruzzi, J.F. Ayala-Zavala, Plant antimicrobials for food quality and safety: recent views and future challenges, Foods 12 (2023) 2315, https://doi.org/10.3390/foods12122315.

[84] A. Papastergiadis, E. Mubiru, H. Van Langenhove, B. De Meulenaer, Malondialdehyde measurement in oxidized foods: evaluation of the spectrophotometric thiobarbituric acid reactive substances (TBARS) test in various foods, J. Agric. Food Chem. 60 (2012) 9589–9594, https://doi.org/10.1021/jf302451c.

[85] F. Shahidi, A. Hossain, Role of lipids in food flavor generation, Molecules 27 (2022) 5014–5024, https://doi.org/10.3390/molecules27155014.

[86] B. Peng, L.L. He, J. Tan, L.T. Zheng, J.T. Zhang, Q.W. Qiao, H.Y. Yuan, Effects of rice aging on its main nutrients and quality characters, J. Agric. Sci. 11 (2019) 44–56, https://doi.org/10.5539/jas.v11n17p44.

[87] M. Zhang, K. Liu, Lipid and protein oxidation of brown rice and selenium-rich brown rice during storage, Foods 11 (2022) 1–14, https://doi.org/10.3390/foods11233878.

[88] S.J. Jadhav, S.S. Nimbalkar, A.D. Kulkarni, D.L. Madhavi, Lipid oxidation in biological and food systems, Food antioxidants: technological, toxicological, and health perspectives (1996) 5–63.

[89] K.A. Youdim, S.G. Deans, H.J. Finlayson, The antioxidant properties of thyme (*Thymus zygis* L.) essential oil: an inhibitor of lipid peroxidation and a free radical scavenger, J. Essent. Oil Res. 14 (2002) 210–215, https://doi.org/10.1080/10412905.2002.9699825.

[90] A.K. Chaudhari, V.K. Singh, S. DasDeepika, B.K. Singh, N.K. Dubey, Antimicrobial, aflatoxin B_1 inhibitory and lipid oxidation suppressing potential of anethole-based chitosan nanoemulsion as novel preservative for protection of stored maize, Food Bioprocess Technol. 13 (2020) 1462–1477, https://doi.org/10.1007/s11947-020-02479-w.

[91] P. Chandravarnan, D. Agyei, A. Ali, Green and sustainable technologies for the decontamination of fungi and mycotoxins in rice: a review, Trends Food Sci. Technol. 124 (2022) 278–295, https://doi.org/10.1016/j.tifs.2022.04.020.